Preparation, coordination and catalytic use of planar-chiral monocarboxylated dppf analogues†

Martin Lamač, Ivana Císařová and Petr Štěpnička*

Received (in Montpellier, France) 20th January 2009, Accepted 25th February 2009
First published as an Advance Article on the web 9th April 2009
DOI: 10.1039/b901262a

A novel polar dppf derivative possessing only planar chirality, 1′,2-bis(diphenylphosphino)-ferrocene-1-carboxylic acid (Hdpc), has been synthesised in racemic form and resolved into enantiomers *via* esters with D-glucose diacetonide (((R_p)- and (S_p)-**3**). (R_p)-Hdpc was further converted to a series of N-substituted amides that were studied as ligands for Pd-catalysed enantioselective allylic alkylation of racemic (*E*)-1,3-diphenylprop-2-en-1-yl acetate or ethyl carbonate with malonate esters, showing high activity and good enantioselectivity (er up to 10 : 90). The catalytic results were correlated with the structural data (X-ray diffraction and solution NMR) for (η^3-allyl)palladium(II) complex (R_p)-[Pd(η^3-1,3-$Ph_2C_3H_3$){Fe(η^5-C_5H_3-1-(C(O)NHCH_2Ph)-2-(PPh_2-κ*P*))(η^5-$C_5H_4PPh_2$-κ*P*)}]ClO_4 (**16**) as a model of the plausible reaction intermediate. A further study into the coordination properties of Hdpc led to isolation of chelate complex [$PdCl_2$(Hdpc-κ^2*P*,*P*′)] (**12**). The crystal structures of *rac*-Hdpc, methyl ester of (R_p)-Hdpc, glycoside (R_p)-**3**, and **12**·Me_2CO suggested a close structural relationship between dppf and Hdpc.

Introduction

Since it was first reported in 1965,[1] 1,1′-bis(diphenylphosphino)-ferrocene (dppf) found manifold uses in coordination chemistry and homogeneous catalysis.[2] The practical success of dppf also stimulated further research into its simple analogues (**I**, Scheme 1)[3] and the related chiral donors (**II**). The chiral derivatives received particular attention, being versatile and efficient ligands for asymmetric metal-mediated reactions.[4]

Despite the enormous amount of research work directed into the area of chiral dppf derivatives, their chemistry is still markedly dominated by BPPFA-type compounds that are readily available in optically pure form from Ugi's amine, FcCH(Me)NMe_2 (Fc = ferrocenyl) *via* directed *ortho*-lithiation[5] and manipulation of the NMe_2 group.[4] In addition to the archetypal BPPFA (**II**, Y = CH(Me)NMe_2),[6,7] a number of related compounds have been reported in which the NMe_2 group was replaced with another donor moiety or the whole aliphatic chain was transformed.[7,8] Other **II**-type compounds still remain uncommon: a ferrocene triphosphine (**II**, Y = PPh_2)[9] and ferrocene diphosphine-oxazolines (**II**, Y = C-chiral 4,5-dihydrooxazolin-2-yl)[4b,10] may serve as typical examples.

The lack of monofunctionalised dissymmetric dppf analogues together with our ongoing interest in the chemistry of ferrocene phosphinocarboxylic ligands[11,12] led us to design a novel monocarboxylic derivative of dppf, 1′,2-bis(diphenylphosphino)ferrocene-1-carboxylic acid (Hdpc in Scheme 1). With its particular disposition of the donor moieties, Hdpc is inherently chiral with the 1,2-disubstituted ferrocene moiety serving as the sole chirality source (*N.B.* The majority of chiral ferrocene ligands **II** possess simultaneously planar and central chirality). Besides, Hdpc fills a gap left between 1′-(diphenylphosphino)ferrocene-1-carboxylic acid (Hdpf),[11,13] its planar chiral isomer, 2-(diphenylphosphino)ferrocene-1-carboxylic acid (**III**),[14,15] and the C_2-symmetric 2,2′-bis(diphenylphosphino)-ferrocene-1,1′-dicarboxylic acid (**IV**, Scheme 1),[16] which have all been studied as donors in asymmetric metal-catalysed organic reactions.

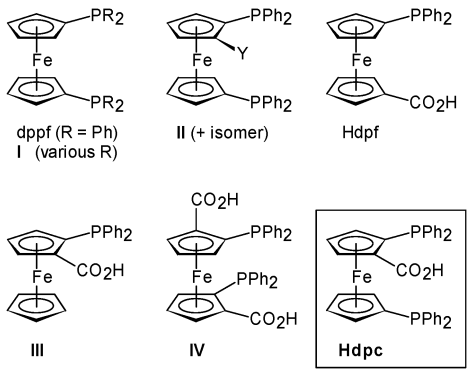

Scheme 1

With this contribution, we describe the synthesis of racemic Hdpc, its resolution into enantiomers and the preparation of a series of enantiopure amides from (R_p)-Hdpc. We also report the preparation and structural characterisation of palladium(II) complexes featuring *rac*-Hdpc and

Department of Inorganic Chemistry, Faculty of Science, Charles University in Prague, Hlavova 2030, Prague 2, 12840, Czech Republic. E-mail: stepnic@natur.cuni.cz; Fax: +420 221 951 253

† Electronic supplementary information (ESI) available: An alternative view of the molecular structure of **12a** (Fig. S1), representative kinetic profile for the alkylation reaction (Fig. S2), geometric data for the glucofuranosyl moiety in (R_p)-**3** (Table S1), and numerical data for the non-linear catalytic study (Table S2). CCDC numbers 700753–700757. For ESI and crystallographic data in CIF or other electronic format see DOI: 10.1039/b901262a

(R_p)-1′,2-bis(diphenylphosphino)-1-(*N*-benzylcarbamoyl)ferrocene as P,P′-chelate ligands and the use of Hdpc-based donors in palladium-catalysed asymmetric allylic alkylation.

Results and discussion

Preparation and characterisation of Hdpc and its amide derivatives

Racemic Hdpc was synthesised (Scheme 2) by sequential lithiation and phosphinylation of 1′,2-dibromoferrocene-1-carboxylic acid (**2**), which was obtained from 1,1′-dibromoferrocene (**1**) as recently reported by Butler and co-workers.[9c] Crude Hdpc typically contains minor amounts of Hdpf and **III**, both resulting from accidental protonolysis of the lithiated intermediate. These acids are chemically similar but, fortunately, could be removed by careful column chromatography. Alternatively, Hdpc was prepared by directed *ortho*-lithiation of Hdpf with *sec*-butyllithium and subsequent phosphinylation (Scheme 2). This route, however, proved rather impractical due to relatively lower isolated yields.

Hdpc was characterised by conventional spectral methods (NMR, IR and MS) and its structure was corroborated by X-ray crystallography. In NMR spectra, Hdpc displays seven ^{1}H and ten ^{13}C resonances attributable to chemically different and/or diastereotopic ferrocene CH and C groups. The presence of non-equivalent PPh_2 moieties is manifested by two sets of signals due to diastereotopic C and CH phenyl protons in the $^{13}C\{^1H\}$ NMR and by two singlets in the $^{31}P\{^1H\}$ NMR spectrum ($CDCl_3$: δ_P −18.2, −18.1; $(CD_3)_2SO$: δ_P −19.0, −17.7). The IR spectrum of Hdpc is dominated by a strong $\nu_{C=O}$ band at 1675 cm^{-1} (*cf.* 1666 cm^{-1} for Hdpf[13]).

The resolution of *rac*-Hdpc was achieved *via* esters with D-glucose diacetonide[14d,17] (Scheme 2). Racemic Hdpc was first reacted with D-glucose diacetonide in the presence of *N*,*N*′-dicyclohexylcarbodiimide and 4-(dimethylamino)pyridine to give a mixture of diastereomeric glucosides **3** along with the urea derivative **4**.[18] The glycoside fraction was separated from **4** by column chromatography and subsequently crystallised from diethyl ether–hexane to afford optically pure (R_p)-**3** in 35% isolated yield (*i.e.*, 70% of the theoretical amount based on *rac*-Hdpc). Chromatographic separation of the combined crystallisation residua afforded optically pure (S_p)-**3**.[19]

The isomeric glycosides and the urea derivative were characterised by elemental analysis and by spectral methods (NMR, IR, and MS). Besides, the configuration of (R_p)-**3** was unequivocally established by X-ray diffraction analysis. In the NMR spectra, the ferrocene signals of (R_p)-**3**, (S_p)-**3** and **4** are observed fully non-equivalent and appear at positions similar to their parent acid. The transformations of the carboxyl group are nicely reflected by changes in the region of the C=O signals. Upon esterification, this resonance shifts to higher fields (*cf.* δ_C 170.13/169.39 for (R_p)/(S_p)-**3**, and 174.80 for Hdpc) while, in the case of urea **4**, it is replaced by two signals at characteristic positions (δ_C 154.36 and 170.71).[18,20] Consistently, the glycosides exhibit their $\nu_{C=O}$ IR bands shifted to higher energies as compared with Hdpc while **4** shows the diagnostic urea bands at 1699 and 1517 cm^{-1}.[18,20]

The NMR parameters of the carbohydrate part in (R_p)-**3** and (S_p)-**3** correspond with those of free D-glucose diacetonide.[21] A notable exception is the splitting of the carbohydrate CH-5″ proton with phosphorus (see Scheme 8), which was confirmed by ^{31}P-decoupled ^{1}H NMR spectra. In view of the structural data revealing a favourable orientation and distance[22] of the interacting molecular parts (P···H^5 3.08 Å, P···H^5–C^5 158°), this splitting can be accounted for a through-space interaction rather than for a long-range scalar coupling.

In the next step, glucofuranosides (R_p)- and (S_p)-**3** were hydrolysed to give the respective Hdpc enantiomers. The hydrolysis was carried out with 1 M KOH in a THF–methanol–water mixture at 50 °C overnight. Subsequent work up afforded optically pure (R_p)- and (S_p)-Hdpc in good isolated yields (76 and 69%, respectively). When the hydrolysis was carried out at room temperature, it did not reach completion. In addition to Hdpc and unreacted glycoside, the reaction mixture contained a minor amount of Hdpc-methyl ester

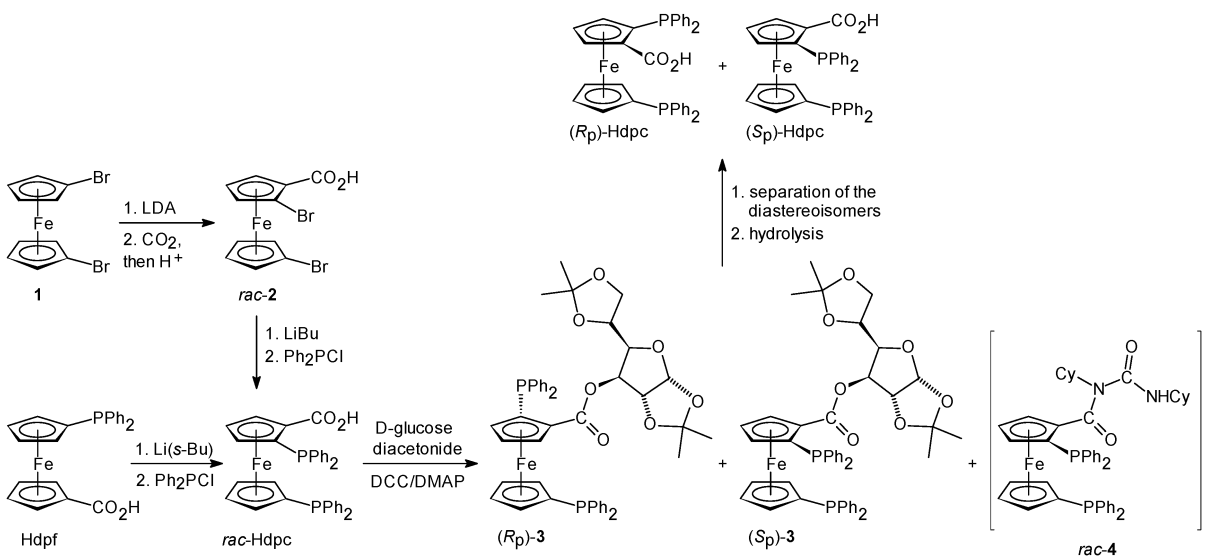

Scheme 2 Preparation and resolution of Hdpc (DCC = *N*,*N*′-dicyclohexylcarbodiimide, DMAP = 4-(dimethylamino)pyridine).

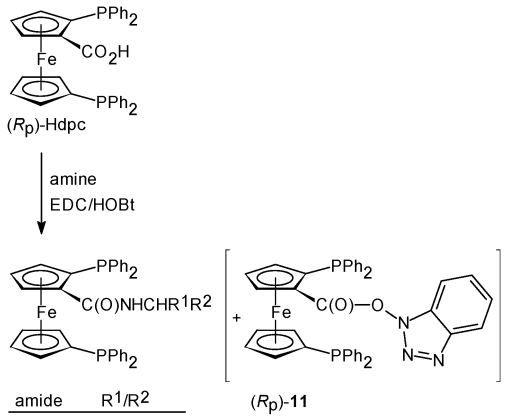

amide	R^1/R^2
(R_p)-**6**	Me/Me
(R_p)-**7**	H/Ph
(R,R_p)-**8**	(*R*)-Me/Ph
(S,R_p)-**8**	(*S*)-Me/Ph
(R_p)-**9**	Ph/Ph
(R_p)-**10**	H/CH_2OH

Scheme 3 Preparation of amides **6–10** (HOBt = 1-hydroxybenzotriazole, EDC = *N*-[3-(dimethylamino)propyl]-*N*′-ethyl-carbodiimide).

((R_p)-**5**), which was isolated and characterised spectroscopically and by X-ray crystallography.

Aiming at utilisation in catalysis, (R_p)-Hdpc was further converted to a series of secondary amides. The series was designed so that both steric properties and chirality of the amide substituents varied (Scheme 3). Amide coupling in the presence of 1-hydroxybenzotriazole and *N*-[3-(dimethylamino)-propyl]-*N*′-ethylcarbodiimide[23,24] proceeded smoothly to give pure amides in good yields. A notable exception was the amidation with benzhydryl amine in the case of which the amide formation was partly hindered by the steric bulk of the amine and some intermediate benzotriazolyl ester (R_p)-**11** was also isolated.[25]

Compounds **6–10** exhibit characteristic amide bands (ν_{NH}, amide I/II) in the IR spectra. Their ^{1}H NMR spectra fully corroborate the formulation by combining the signals of the phosphinoferrocene moiety with those due to the nitrogen substituents. It is worth noting that despite the non-degenerate nature of the NMR signals, the spectra may turn deceptively simple. For instance, the ^{1}H NMR spectrum of (R_p)-**7** recorded in $CDCl_3$ showed the PhCH_2 protons as a doublet resulting from interaction with the NH proton (Fig. 1). When the spectrum was recorded in C_6D_6, the same signal was observed as a pair of double doublets as expected for diastereotopic CH_2 protons interacting with an NH group ($^2J_{HH}$ = 14.9, $^3J_{HH}$ = 5.9 Hz). The ferrocene signals also became better resolved in the latter solvent. ^{31}P NMR data of **6–10** do not differ much from those of Hdpc. However, the individual signals are better separated ($\Delta\delta_P$ = 2.0–2.8 ppm, *cf.* $\Delta\delta_P$ = 0.1 ppm for Hdpc in $CDCl_3$).

The crystal structures of *rac*-Hdpc, ester (R_p)-5 and glycoside (R_p)-3

Crystal structures of *rac*-Hdpc, (R_p)-**5** and (R_p)-**3** were determined by single-crystal X-ray diffraction. Views of the molecular structures are shown in Fig. 2–4. Selected geometric data for the acid are given in the figure caption while those for (R_p)-**5** and (R_p)-**3** are presented in Table 1.

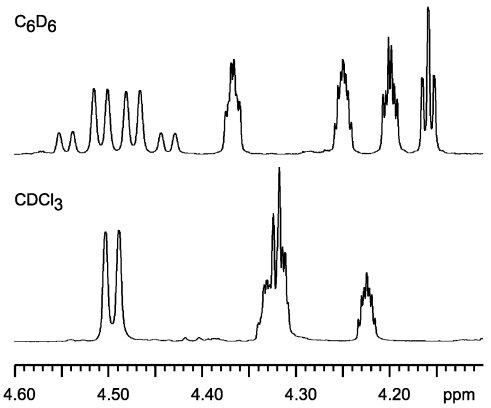

Fig. 1 Proton NMR spectra of (R_p)-**7** as recorded in C_6D_6 (top) and in $CDCl_3$ (bottom) at 25 °C. In both cases, three ferrocene CH resonances fall outside the range indicated.

The overall molecular structure of *rac*-Hdpc (Fig. 2a) and, consequently, its crystal packing seems to be dictated largely by the bulky peripheral phosphino groups and by a tendency to attain a higher symmetry (inversion centre). As a result, the 'embedded' carboxyferrocenyl moiety is disordered over two

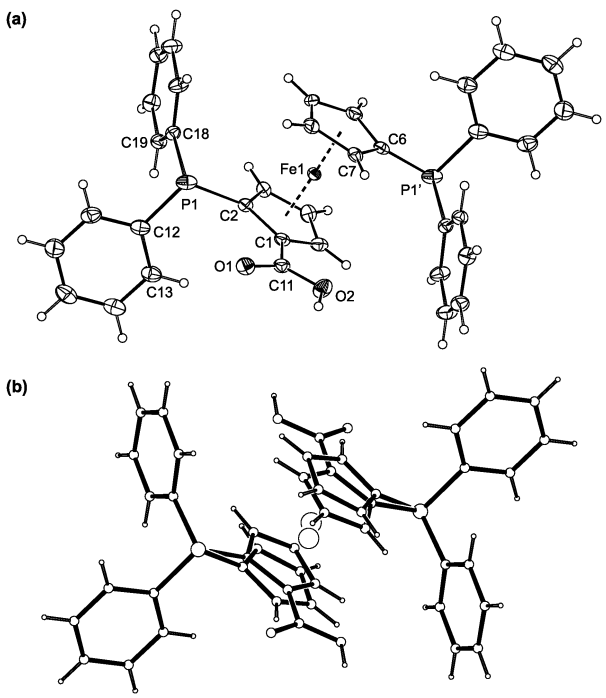

Fig. 2 (a) View of the molecular structure of *rac*-Hdpc, showing the atom labelling scheme and displacement ellipsoids at the 30% probability level [the (R_p) component is shown]. (b) Superposition of both orientations encountered in the crystals of *rac*-Hdpc. Selected distances and angles: Fe1–Cg1 1.66(3), Fe1–Cg2 1.64(3) Å, ∠Cp1,Cp2 1.0(3)°; C11–O1 1.233(4), C11–O2 1.309(4), C1–C11 1.450(5) Å; O1–C11–O2 124.1(3)°; C2–P1 1.964(7)/C6–P1′ 1.683(9), P1–C12 1.837(2), P1–C18 1.833(2) Å. Primed atoms are generated by the crystallographic (1 − *x*, −*y*, −*z*) symmetry operation. For definition of the ring planes, see Table 1.

inversion-related positions (enantiomers; Fig. 2b), which underscores structural similarity between Hdpc and dppf.[26,27]

Geometric data for *rac*-Hdpc do not depart significantly from those reported for dppf,[27] Hdpf,[13] 2-(diphenylphosphinoyl)-ferrocene-1-carboxylic acid[14c] and its corresponding alcohol,[28] particularly when the relatively lower precision of the geometry determination for the disordered ferrocene scaffold is considered. The adjacent phosphine and carboxyl groups do not impart any notable deformation to their bonding cyclopentadienyl ring Cp1 as evidenced by the torsion angle C11–C1–C2–P1 = 3.1(9)° but the carboxyl plane is rotated from the Cp1 plane by 10.1(5)°.

Similarly to Hdpf,[13] individual molecules of *rac*-Hdpc associate into dimers *via* centrosymmetric double hydrogen bridges between their carboxyl groups (O1···O2 2.630(3) Å; angle at H = 168°). Because of the disorder, the hydrogen-bonded pairs can be described equally well as being composed either of the molecule and its inverted image or, alternatively, of the molecule and the other contributing component translated in the crystallographic *a* direction.

Structural data for ester (R_p)-**5** also compare well with those of dppf[27] and Hdpf methyl ester.[13] The cyclopentadienyl (Cp) rings are mutually tilted only by 0.6(1)° and the Fe–ring centroid distances are similar. The ferrocene moiety does not exert any torsional deformation at the C1–C2 bond, yet the substituents bind somewhat asymmetrically.[29] The diphenylphosphino groups assume a staggered antiperiplanar conformation with τ = 178°. Even though the crystals of (R_p)-**5** are chiral (space group $P2_1$), such molecular conformation results in an apparent pseudoinversion symmetry, which is violated only by the carboxyl substituent (compare the unit cell parameters of *rac*-Hdpc and (R_p)-**5**).

The structure of glycoside (R_p)-**3** (Fig. 4) is not unexpected in view of the structural data of *rac*-Hdpc and (R_p)-**5** (Table 1). When compared with the latter compound, (R_p)-**3** shows a somewhat higher tilt of the ferrocene cyclopentadienyls and rotation of the carboxyl plane. The most notable difference, however, is seen in the conformation of the ferrocene moiety, which is near to *anti*-eclipsed. The geometry of the 1,2:5,6-di-*O*-isopropylidene-α-D-3-gluco-furanosyl moiety (see Table S1, ESI†) compares favourably to that reported for the related derivatives of organic acids.[30]

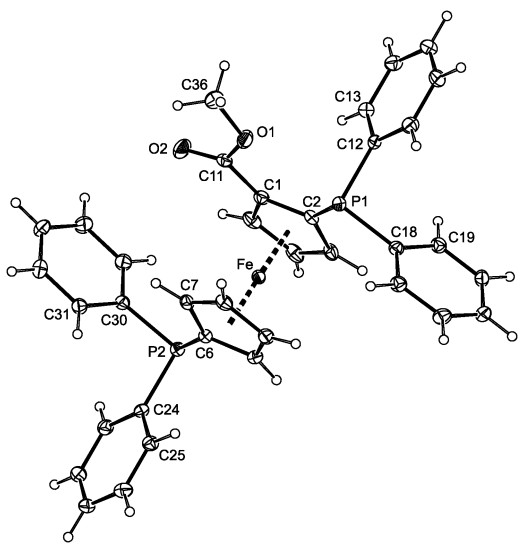

Fig. 3 View of the molecular structure of ester (R_p)-**5**. Displacement ellipsoids enclose the 30% probability level.

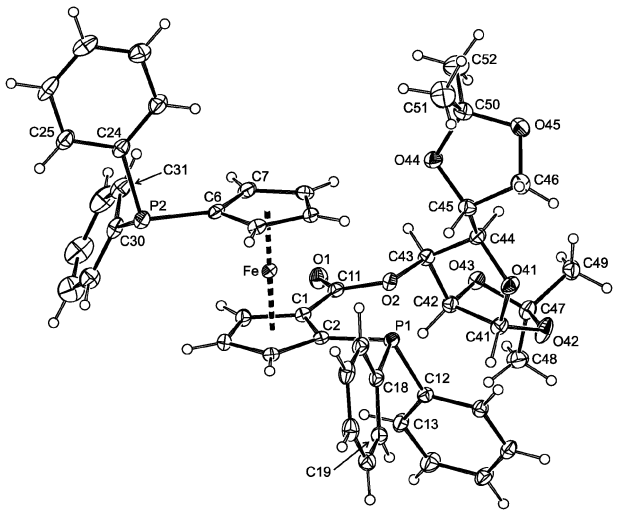

Fig. 4 View of the molecular structure of (R_p)-**3** showing displacement ellipsoids at the 30% probability level. An alternative view of the glucofuranosyl part and selected geometric data are available as ESI†.

Table 1 Selected distances and angles for (R_p)-**5** and (R_p)-**3** (in Å and °)[a]

Compound	(R_p)-**5**[d]	(R_p)-**3**[e]
Fe–Cg1	1.6493(9)	1.645(1)
Fe–Cg2	1.6529(9)	1.656(1)
∠Cp1, Cp2	0.6(1)	2.5(2)
C11–C1–C2–P1	4.9(3)	3.2(4)
τ[b]	178	154
C1–C11	1.474(3)	1.465(4)
C11–O1	1.200(3)	1.209(3)
C11–O2	1.338(3)	1.356(3)
O1–C11–O2	123.4(2)	123.0(2)
φ[c]	8.0(2)	11.0(3)
P1–C2	1.825(2)	1.833(3)
P2–C6	1.826(2)	1.813(2)

[a] The ring planes are defined as follows: Cp1 = C(1–5), Cp2 = C(6–10); Cg1 and Cg2 are the respective ring centroids. [b] Torsion angle C2–Cg1–Cg2–C6. [c] Dihedral angle of the {C11,O1,O2} and Cp1 least-squares planes. [d] Other data: O2–C36 1.439(3) Å; C11–O2–C36 117.4(2)°. [e] For data describing the glucofuranosyl moiety, see ESI†, Table S1.

Synthesis and characterisation of complex 12

Reaction of *rac*-Hdpc with [$PdCl_2$(cod)] (cod = η^2:η^2-cycloocta-1,5-diene) in chloroform afforded chelate complex *rac*-[$PdCl_2$(Hdpc-κ^2P,P')] (**12**) as an orange, poorly soluble microcrystalline solid (Scheme 4). X-Ray quality crystals of the solvate *rac*-[$PdCl_2$(Hdpc-κ^2P,P')]·Me_2CO (**12a**) were grown by diffusion of [$PdCl_2$(cod)] in acetone into a solution of the acid in $CHCl_3$.

NMR spectra of **12** are in accordance with the formulation, showing one set of ferrocene signals. The spectra also suggest P,P-chelate coordination of the ligand *via* a shift of the

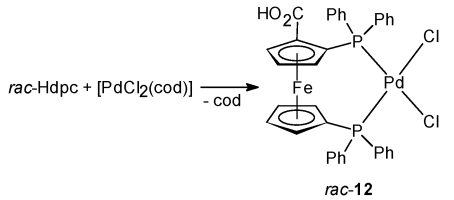

Scheme 4 Preparation of palladium(II) complex **12**.

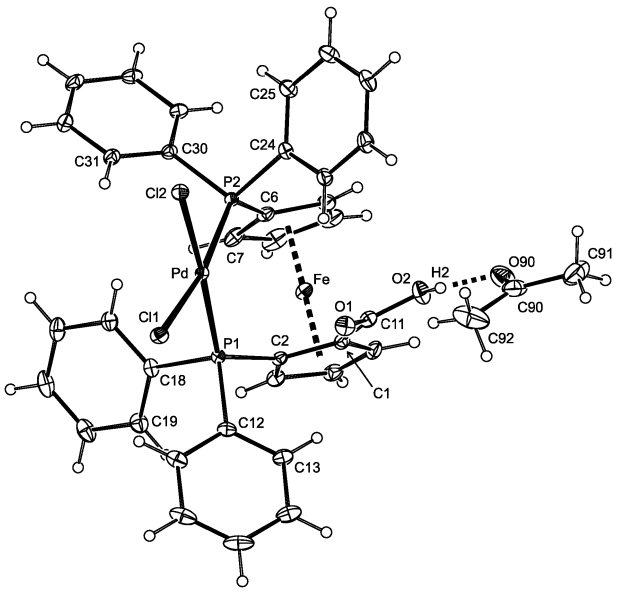

Fig. 5 View of the molecular structure of **12a** showing the atom labelling scheme and displacement ellipsoids at the 30% probability level. Hydrogen bond between the carboxyl OH group and the solvate is indicated with a dotted line (O2···O90 = 2.621(3) Å, angle at H2 = 156°).

^{31}P NMR signals to lower fields (δ_P 33.5 and 43.7) and, above all, their mutual coupling ($^2J_{PP}$ = 35 Hz). The $\nu_{C=O}$ band is observed at 1703 cm^{-1}, *i.e.* shifted by about 30 cm^{-1} to higher energies *vs.* solid Hdpc.

The crystal structure of solvate **12a** was established by X-ray diffraction analysis (Fig. 5, Table 2). Coordination geometry around the palladium is generally similar[31] to that reported for [PdCl$_2$(dppf-κ^2*P*,*P*′)]·S, where S = CH_2Cl_2,[32] and $CHCl_3$.[33] The coordination environment around palladium is *cis* square-planar, with the palladium and its four ligating atoms being coplanar within 0.055 Å.[34] The Pd–donor distances are quite similar but the interligand angles differ from the ideal 90°. The P1–Pd–P2 (or the ligand bite angle) is the most opened. Nonetheless, this opening seems to be well compensated by in-plane closure of the remaining angles as the sum of the interligand angles (359.85°) rules out any pronounced tetrahedral distortion. The geometry of the ferrocene moiety in **12a** remains largely unchanged upon coordination[35] but the ligand molecule undergoes a pronounced conformational change. In order to allow for chelate formation, the phosphorus groups are rotated closer to each other to a position roughly halfway between *syn*-eclipsed and *syn*-staggered (τ = 26°). The coordination plane and the ferrocene unit are tilted at the dihedral angle of the Cp1 and PdL$_4$ planes of 67.1(1)° (see Fig. S1, ESI†).

Table 2 Selected distances and angles for **12a** (in Å and °)[a,b]

Distances		Angles	
Pd–Cl1	2.3379(6)	Cl1–Pd–Cl2	87.27(2)
Pd–Cl2	2.3390(6)	Cl1–Pd–P1	88.76(2)
Pd–P1	2.2912(6)	Cl2–Pd–P2	83.47(2)
Pd–P2	2.2822(6)	P1–Pd–P2	100.35(2)
Fe–Cg1	1.629(1)	PdL$_4$ *vs.* Cp1[c]	67.1(1)
Fe–Cg2	1.643(1)	∠ Cp1,Cp2	2.3(2)
P1–C2	1.803(2)	C11–C1–C2–P1	1.4(3)
P2–C6	1.809(2)	τ[d]	26
C11–O1	1.209(3)	O1–C11–O2	124.4(2)
C11–O2	1.338(3)	φ[d]	17.4(3)

[a] Definition of the ring planes: Cp1 = C(1–5), Cp2 = C(6–10); Cg1 and Cg2 denote the respective ring centroids. [b] Data for the solvent molecule: C90–O90 1.208(4), C90–C91 1.504(4), C90–C92 1.466(6) Å; C91–C90–C92 119.6(3)°. [c] The dihedral angle of the {Pd,Cl1, Cl2,P1,P2} and Cp1 planes. [d] Parameters τ and φ are defined as for free ligands (see Table 1).

Catalytic tests

Glycosides (R_p)- and (S_p)-**3** and the donors relating to (R_p)-Hdpc (the acid and all amides shown in Scheme 2) have been studied as ligands for palladium-catalysed asymmetric allylic alkylation (Scheme 5)[36] of (*E*)-1,3-diphenylprop-2-en-1-yl acetate (**13a**) or its corresponding ethyl carbonate **13b** with C-anions generated from dialkyl malonates and *N*,*O*-bis-(trimethylsilyl)acetamide in the presence of alkali metal acetates.[37] The reactions were usually carried out in dichloromethane at room temperature using 3 mol% of Pd-catalyst formed *in situ* from the respective ligand and [{Pd(μ-Cl)(η^3-C_3H_5)}$_2$] (Pd : ligand = 1 : 1).

The experiments with (*S*,R_p)-**8** suggested that the alkylation reaction with dimethyl malonate is typically completed within 1 h (for a representative kinetic profile, see Fig. S2, ESI†) and its stereochemical outcome (ee)[38] is perfectly reproducible. Nevertheless, the reaction times were uniformly set to 20 h in order to minimise a bias due to varying induction periods and different reactivity of the C-nucleophiles tested (dimethyl *vs.* di-*tert*-butyl malonate).

Another series of reactions performed with the mixtures of isomeric ligands (R_p)-**3** and (S_p)-**3** excluded major non-linear effects[39] operating in the catalytic system (Fig. 6). The $ee_{product}$ was always proportional to de_{ligand} within the experimental error (*ca.* ±1% ee), which points to a dominating role of planar chirality. Indeed, this observation is in line with the structural data (see below) indicating that Hdpc-based ligands coordinate to palladium as P,P′-chelate donors. Thus, although chiral, the glucofuranosyl groups (R_p)-**3** and (S_p)-**3** act as 'innocent', sterically demanding groups that only direct

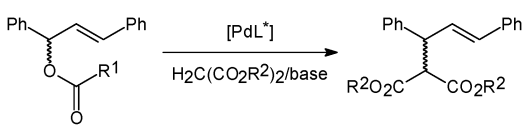

13a (R^1 = Me)
13b (R^1 = OEt)

14a (R^2 = Me)
14b (R^2 = *t*-Bu)

Scheme 5

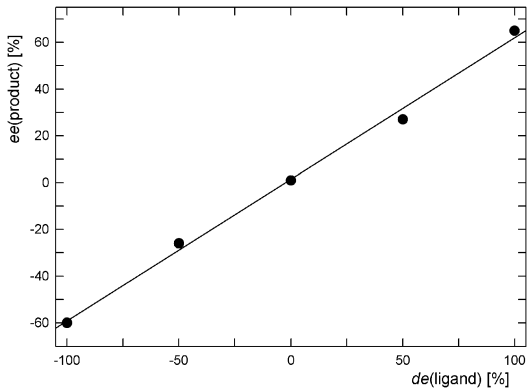

Fig. 6 Variation of asymmetric induction ($ee_{product}$) as a function of de for the mixture of diastereomeric ligands (R_p)- and (S_p)-**3** in allylic alkylation of **13a** with dimethyl malonate. Parameters of the linear fit: $ee_{product} = 0.61(2)\ de_{ligand} + 1(2)$ ($r^2 = 0.996$); for numerical data, see ESI† (Table S2).

access of the nucleophile towards the η^3-allyl intermediate (*vide infra*).

The results obtained with various ligands (Table 3) indicate that the conversion of the carboxyl to a carboxamido group has a beneficial effect on the ee. On the other hand, the stereochemical course was rather insensitive to the substitution at the amide nitrogen (even for the functionalised amide (R_p)-**10**). The amides bearing the 1-phenylethyl substituents, (R,R_p)-**8** and (S,R_p)-**8**, represented a typical example of matched and mismatched chirality. Whereas the (*R*)-1-phenylethyl derivative showed the lowest ee among the amides, approaching that achieved with (R_p)-Hdpc itself, its diastereoisomer (S,R_p)-**8** gave the alkylation product with the highest ee. Notably, when preformed complex [Pd(η^3-1,3-$Ph_2C_3H_3$){(R_p)-**7**-κ^2P,P'}]ClO_4 ((R_p)-**16**; *vide infra*) was employed as the 'catalyst', the ee was considerably lower than with the corresponding catalyst generated *in situ* (Table 3, entries 5 and 10).

In attempts at improving the stereoselectivity, the catalytic system based on (S,R_p)-**8** as the best ligand was varied by changing the base additive, the nucleophile and the reaction temperature (Table 4). Reactions performed without any alkali metal acetate or in the presence of LiOAc gave significantly lower ee's than those carried out with all other salts (Na–Cs). The variation among the heavier alkali metal acetates was negligible. A lowering of the reaction temperature to 0 °C or the use of **13b** as a substrate did not improve the reaction selectivity either. An increase in ee was achieved with a more sterically demanding nucleophile (di-*tert*-butyl malonate), though in different extent for the different ligands (Table 4).

Table 3 Survey of the chiral ligands in palladium-catalysed asymmetric allylic alkylation[a]

Entry	Ligand	Ee (%) [config]
1	(R_p)-Hdpc	+54 [*R*]
2	(R_p)-**3**	+65 [*R*]
3	(S_p)-**3**	−60 [*S*]
4	(R_p)-**6**	+60 [*R*]
5	(R_p)-**7**	+60 [*R*]
6	(R,R_p)-**8**	+55 [*R*]
7	(S,R_p)-**8**	+67 [*R*]
8	(R_p)-**9**	+58 [*R*]
9	(R_p)-**10**	+58 [*R*]
10	Complex[b]	+49 [*R*]

[a] The alkylation of **13a** was performed with dimethyl malonate–BSA mixture (both 3 equiv. with respect to **13a**) in the presence of catalytic amount of NaOAc (6 mol% with respect to **13a**) and 3 mol% of Pd-catalyst generated *in situ* from [{Pd(μ-Cl)(η^3-C_3H_5)}$_2$] and the ligand (Pd : ligand = 1). The results are an average of two independent runs. The conversions determined by ^{1}H NMR spectroscopy were quantitative in all cases. For details, see Experimental. [b] The reaction was performed in the presence of 3 mol% of (R_p)-**16**.

Table 4 Optimisation of the reaction conditions with ligand (S,R_p)-**8**[a]

Entry	*T*/°C	Ligand	Substrate	Base	Ee (%) [config]
1	22	(S,R_p)-**8**	**13a**	LiOAc	+52 [*R*]
2	22	(S,R_p)-**8**	**13a**	NaOAc	+67 [*R*]
3	22	(S,R_p)-**8**	**13a**	KOAc	+66 [*R*]
4	22	(S,R_p)-**8**	**13a**	RbOAc	+68 [*R*]
5	22	(S,R_p)-**8**	**13a**	CsOAc	+68 [*R*]
6	22	(S,R_p)-**8**	**13a**	None	+57 [*R*]
7	0	(S,R_p)-**8**	**13a**	NaOAc	+67 [*R*]
8	22	(S,R_p)-**8**	**13b**	NaOAc	+65 [*R*]
9[b]	22	(S,R_p)-**8**	**13a**	NaOAc	+80 [*R*]
10[b]	22	(R,R_p)-**8**	**13a**	NaOAc	+77 [*R*]
11[b]	22	(R_p)-**7**	**13a**	NaOAc	+63 [*R*]

[a] The alkylation of **13a** and **13b** was performed with a mixture of the respective dialkyl malonate (3 equiv.), BSA (3 equiv.) in the presence of catalytic amount of NaOAc (6 mol% with respect to the allylic substrate; if appropriate) and 3 mol% of Pd-catalyst generated *in situ* from [{Pd(μ-Cl)(η^3-C_3H_5)}$_2$] and the ligand (Pd : ligand = 1).The conversions were quantitative with the exception of entries 9 (conv. 93%) and 11 (conv. 88%). For detailed conditions, see Experimental. [b] The reaction was performed with di-*tert*-butyl malonate as the nucleophile.

Preparation and crystal structure of the model complex (R_p)-16—mechanistic implications

In order to gain a structural insight into the factors controlling the stereochemistry of the alkylation reaction, η^3-1,3-diphenylallyl complex (R_p)-**16** was synthesised and structurally characterised as a model for the plausible reaction intermediate. The compound smoothly resulted by bridge-cleavage of dimer **15** followed by halide abstraction with silver(I) perchlorate (Scheme 6). Evaporation of the reaction mixture afforded essentially pure product (≥ 90% according to NMR; Fig. 7) in good yield.

The composition of the cation in (R_p)-**16** was established from high-resolution mass spectra whilst the presence of the perchlorate counterion was confirmed by its ν_3 (1097 cm^{-1}) and ν_4 bands (624 cm^{-1}) in the IR spectrum. Although the

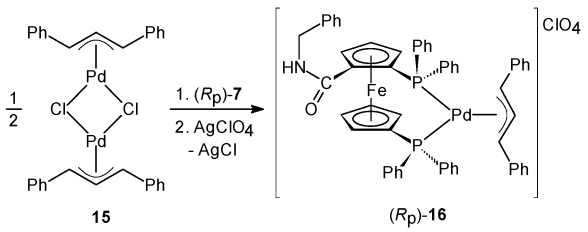

Scheme 6

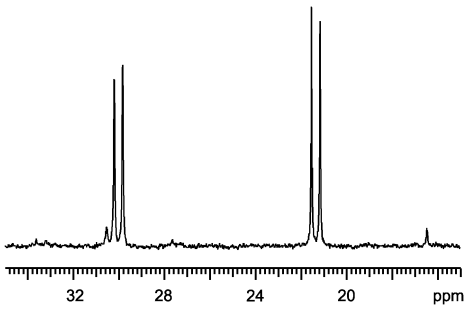

Fig. 7 $^{31}P\{^{1}H\}$ NMR spectrum of crude (R_p)-**16** ($CDCl_3$, 25 °C). The doublets integrate to the same value.

NMR spectra of (R_p)-**16** could be analysed only partly due to extensive signal overlaps, they provided valuable information about the coordination of the ferrocene ligand. For instance, $^{31}P\{^{1}H\}$ NMR spectrum (Fig. 7) displayed a pair of doublets with $^{2}J_{PP}$ = 61 Hz, indicating that (R_p)-**7** coordinates as a P,P′-chelate. The fact that the amide group is not involved in coordination was inferred from a negligible coordination shift of the ^{13}C NMR signal of the CONH group ($\Delta\delta_C$ = 0.5 ppm) and nearly intact amide bands in the IR spectrum. The resonances due to the η^3-1,3-diphenylallyl ligand were observed in the expected region[40] but with only a minor differentiation between the allylic termini [$\Delta\delta_H \approx 0.6$, $\Delta\delta_C$ = 2.4; *cf.* the data for donor-dissymmetric complexes in ref. 40]. Actually, this observation is hardly surprising in view of the donor-symmetric nature of (R_p)-**7** which in turn implies that the stereochemical course of the reactions is controlled predominantly by steric factors.

Crystals of (R_p)-**16**·2CH_3CO_2Et ((R_p)-**16a**) suitable for X-ray diffraction analysis resulted upon crystallisation of the complex from ethyl acetate. However, the solvent molecules were disordered in structural voids and their contribution was subtracted from the overall diffraction pattern (see Experimental). A view of the cation in (R_p)-**16a** is shown in Fig. 8 and selected geometric parameters are presented in Table 5.

The crystal structure reveals the diphenylallyl ligand in (R_p)-**16a** to have a *syn–syn* conformation and to assume an *exo* orientation *vs.* the carbamoyl group. The allyl plane {C43,C44,C45} is rotated by 65.3(6)° from the {Pd,P1,P2} plane so that the central C44 atom is closest to the palladium. The coordination geometry around the palladium atom is quite symmetric in both Pd-donor distance and interligand angles and generally corresponds with that reported for [Pd(η^3-1,3-$Ph_2C_3H_3$)(L-κ^2*P*,*P*′)]BF_4·C_6H_6, where L is (*S*,*S*)-1,1′-bis{phenyl(1-naphthyl)phosphino}ferrocene.[41]

Despite the symmetry of the coordination environment, the 1,3-diphenylallyl moiety is considerably twisted. This is a likely consequence of steric constraints imposed by the bulky PPh_2 groups, forcing the phenyl rings at η^3-allyl group away from the ferrocene ligand. This torsion is manifested by the torsion angles C44–C43–C46–C(47/51) = 33.1(8)/−142.8(6)° and C44–C45–C52–C(53/57) = −19.1(9)/157.0(6)°, departing notably from 0/180° for an ideal all-in-plane conformation. The phenyl rings C(46–51) and C(52–57) are mutually rotated by 38.0(3)°. Nonetheless, such deformation need not

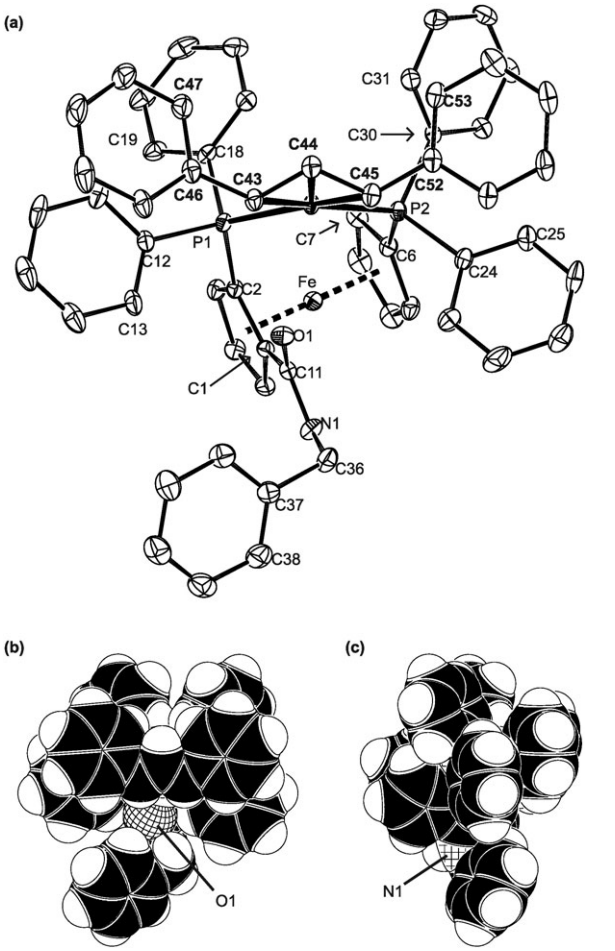

Fig. 8 (a) View of the cation in the structure of (R_p)-**16a** showing the atom-labelling scheme (20% displacement ellipsoids). For clarity, the hydrogen atoms are omitted and atomic labels of the allyl ligand are shown in bold. (b, c) Space filling models of the cation as viewed perpendicular to the allyl plane (b) and along the C43–C45 vector (c).

Table 5 Selected distances and angles for (R_p)-**16a** (in Å and °)[a]

Distances		Angles	
Pd–P1	2.344(1)	P1–Pd–P2	102.54(5)
Pd–P2	2.330(1)	P1–Pd–C43	96.2(1)
Pd–C43	2.256(5)	P2–Pd–C45	94.8(1)
Pd–C44	2.181(6)	P1–Pd–C44	128.6(2)
Pd–C45	2.226(6)	P2–Pd–C44	127.3(1)
C43–C44	1.384(7)	C43–Pd–C45	66.2(2)
C44–C45	1.395(8)	C43–C44–C45	123.4(6)
C43–C46	1.456(8)	C46–C43–C44	123.6(6)
C45–C52	1.480(8)	C52–C45–C44	122.7(6)
Fe–Cg1	1.640(2)	Allyl *vs.* {PdP_2}[b]	65.3(6)
Fe–Cg1	1.640(3)	∠ Cp1,Cp2	2.3(3)
P1–C2	1.824(6)	C11–C1–C2–P1	6.7(7)
P2–C6	1.804(5)	τ[c]	30
C11–O1	1.230(7)	O1–C11–N1	121.9(4)
C11–N1	1.328(8)	φ[d]	6.5(6)

[a] Definition of the ring planes: Cp1 = C(1–5), Cp2 = C(6–10); Cg1 and Cg2 denote the respective ring centroids. [b] Dihedral angle of the planes {C43,C44,C45} and {Pd,P1,P2}. [c] Torsion angle C2–Cg1–Cg2–C6. [d] Dihedral angle of the {C11,O1,N1} and Cp1 least-squares planes.

necessarily destabilise the structure. In the present case, it seems to aid the generation of conformation-stabilising offset π···π stacking interactions[42] between phenyl rings of the allyl ligand and the PPh_2 moieties. The planes of the phenyl rings C(46–51) and C(12–13) are tilted by 2.4(4)° and the distance of the ring centroids is 3.684(5) Å, which is very similar to centroid separation in α-graphite.[43] The arrangement at the other allyl terminus is less favourable but still allows for π···π interaction between the rings C(52–57) and C(24–29) (dihedral angle = 22.9(3)°, centroid separation = 4.408(5) Å).

Similarly to **12a**, the formation of (R_p)-**16a** leaves the ligand geometry mostly unchanged except for conformational reorganisation. Chelate coordination brings the phosphorus substituents to an intermediate conformation, close to *syn*-staggered (τ = 30°; the ideal value is 36°). The ferrocene unit is tilted by 2.3(3)°, exerts identical Fe–ring centroid distances and symmetrically binds its functional substituents.

Assuming that the complex geometry remains largely unchanged during the reaction (*viz.* least-motion principle[44]) and that the ligand does not electronically differentiate the allylic termini, the attack of the nucleophile can be expected to occur preferentially from the less sterically hindered site, *i.e.* at the carbon atom *trans* to phosphorus at the disubstituted Cp ring (atom C45 in Fig. 8a). According to the generally accepted mechanism,[36] this would lead to the (*R*)-configured product, which is indeed in line with the reaction outcome (Scheme 7). The other, minor isomer may result from attack at the second allylic terminus or by isomerisation of the reaction intermediates as it is typical for allyl complexes. All other isomeric η^3-allyl complexes, including the second most probable *endo–syn–syn* η^3-allyl intermediate, are probably less favoured for steric reasons and because of (partial) loss of stabilisation through π···π interactions. The same very likely applies also to the Pd(η^2-alkene) intermediates (Scheme 7) directly resulting from the attack of the nucleophile.

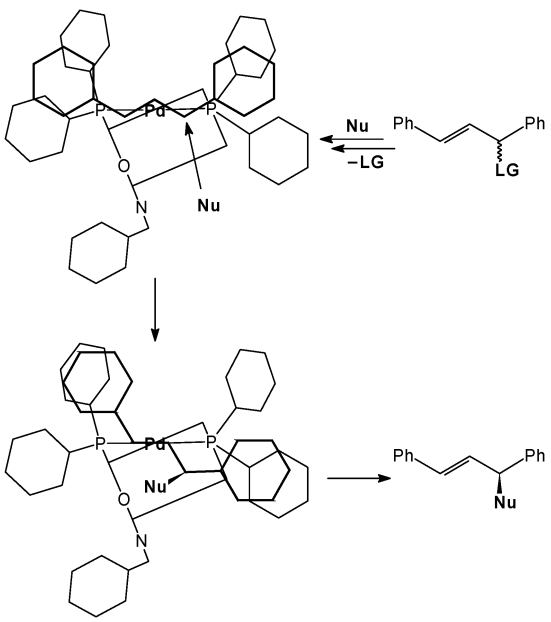

Scheme 7 Plausible reaction mechanism (Nu = nucleophile, LG = leaving group).

Conclusions

1′,2-Bis(diphenylphosphino)ferrocene-1-carboxylic acid (Hdpc) is a novel, planar-*only* chiral monofunctionalised derivative of dppf, accessible in both enantiomeric forms *via* esters with D-glucose diacetonide. The available data indicate that Hdpc and dppf are structurally similar and show similar coordination properties. Not surprisingly, the ee's achieved with Hdpc-based ligands in palladium-catalysed asymmetric allylic alkylation fall into the range reported for BPPFA-like[4f,8a,36f] and oxazolinyl-substituted dppf analogues.[4b,10]

The data so far collected during testing of chiral ferrocene phosphino-carboxylic donors in asymmetric allylic alkylation (ref. 15*a–d* and 16 and this work) consistently indicate that phosphinocarboxamides are better ligands for this reaction than their parent acids,[45] and that planar chirality is the key factor determining their catalytic efficiency. The rationale for the somewhat lower ee's attained with Hdpc-amides as compared to amides based on **III** and **IV** (Scheme 1) can be sought in their particular ligating properties (the number and type of the donor atoms and their spatial distribution). First, Hdpc-based ligands coordinate to palladium as practically symmetric P,P-chelates and, hence, do not provide sufficient electronic differentiation of the enantiotopic allylic termini such in **III**-based amides that form P,O-chelates.[15c] Second, the amide substituents are rather far away from the Pd(η^3-allyl) unit and thus cannot efficiently control the access of the nucleophile towards the coordinated allyl moiety. This unfavourable situation could be improved (in principle) by increasing the donor-asymmetry of Hdpc *via* different substituents at the phosphorus atoms[46] or by introduction of a second directing moiety such in C_2-symmetric ligands based on acid **IV**.[16]

Experimental

Materials and methods

The syntheses were performed under an argon atmosphere with exclusion of the direct daylight. Tetrahydrofuran was distilled from sodium–benzophenone ketyl. Acetone, dichloromethane and chloroform were dried over K_2CO_3 and distilled. Acetonitrile was dried over P_2O_5 and distilled. Methanol was distilled. Chloro-diphenylphosphine was distilled under vacuum. Acid **2**,[9c] 1,3-diphenylprop-2-en-1-yl acetate (**13a**),[47] ethyl (1,3-diphenylprop-2-en-1-yl) carbonate (**13b**),[48] and di-μ-chlorido-bis(η^3-1,3-diphenylallyl)dipalladium(II) (**15**)[49] were prepared following the literature procedures. Other chemicals and solvents used in workup and in crystallisations were used as received (Fluka and Aldrich).

NMR spectra were recorded with a Varian Unity Inova 400 spectrometer at 25 °C. Chemical shifts (δ/ppm) are given relative to internal $SiMe_4$ (^{13}C and ^{1}H) or to external 85% aqueous H_3PO_4 (^{31}P). The assignment of the NMR signals is based on conventional 1D and 2D (COSY, ^{13}C gHSQC and ^{13}C gHMBC) spectra. In addition to the standard notation of the signal multiplicity, vt and vq are used to distinguish virtual multiplets arising in the spin systems of the substituted cyclopentadienyl (Cp) rings (Cy = cyclohexyl). Labelling schemes for Hdpc and glycosides **3** are presented in

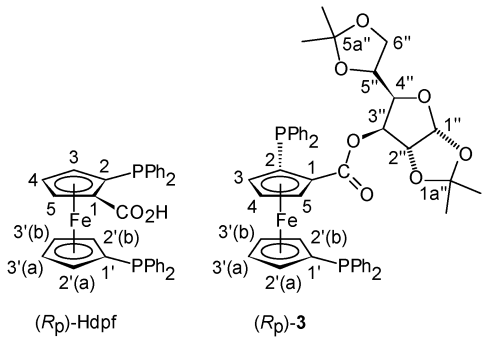

Scheme 8 The labelling scheme adopted for (R_p)-Hdpc and (R_p)-**3**. The (S_p)-isomers are labelled analogously.

Scheme 8. IR spectra were recorded on an FT-IR Nicolet Magna 650 spectrometer. Electrospray (ESI) mass spectra were measured with a Thermo Scientific LTQ Orbitrap XL or with a Bruker Esquire 3000 (only low-resolution spectra) spectrometers. The composition of the ionic species was corroborated by a comparison of the experimental and calculated isotopic patterns. Optical rotations were determined on an Autopol III polarimeter (Rudolph Research) at room temperature. Melting points were determined on a Kofler block.

Syntheses

Racemic 1′,2-bis(diphenylphosphino)ferrocene-1-carboxylic acid (*rac*-Hdpc). *n*-Butyllithium (10 mL, 2.5 M in hexanes, 25 mmol) was added dropwise to a solution of *rac*-1′,2-dibromoferrocene-1-carboxylic acid (**2**; 2.77 g, 7.14 mmol) in THF (60 mL) with stirring and cooling to −78 °C whereupon the colour of the reaction mixture changed from orange to red. The mixture was stirred at −78 °C for 2 h, and treated with $ClPPh_2$ (3.0 mL, 16.7 mmol). Stirring was continued at −78 °C for 30 min and then at room temperature for 18 h. Then, the reaction solution was mixed with 5% aqueous KOH (50 mL) and the volatiles were removed under vacuum. The heterogeneous residue (aqueous phase containing an oily material) was extracted with diethyl ether (2 × 30 mL) and then acidified with concentrated phosphoric acid (to pH ≈ 2). The precipitated product was dissolved by addition of THF, the organic phase was separated and the aqueous layer was extracted with THF (3 × 50 mL). The combined organic solutions were washed with brine, dried over $MgSO_4$ and evaporated under vacuum. The residue was purified by column chromatography on silica gel (several runs). Elution with dichloromethane–methanol (10 : 1 v/v) followed by evaporation of the first fractions afforded pure *rac*-Hdpc as an orange solid. Combined yield: 2.24 g (52%). The combined residua (total 1.25 g) contained *rac*-Hdpc, Hdpf and *rac*-2-(diphenylphosphino)ferrocenecarboxylic acid in *ca.* 1 : 3 : 4 molar ratio according to NMR spectra.

Analytical data for rac-*Hdpc*. Mp dec. above 190 °C. ^{1}H NMR ($CDCl_3$): δ 3.63 (ddd, J = 2.5, 1.5, 0.8 Hz, 1 H, CH-3), 3.88 and 4.30 (2 × d of vq, 1 H, CH-2′), 4.34 (vt, J = 2.5 Hz, 1 H, CH-4), 4.51 and 4.53 (2 × d of vq, 1 H, CH-3′); 5.00 (m, 1 H, CH-5), 7.10–7.46 (m, 20 H, P*Ph*$_2$). ^{13}C{^{1}H} NMR ($CDCl_3$): δ 74.35 (d, $^1J_{PC}$ = 15 Hz, C-2), 74.80 (d, J_{PC} = 12 Hz, CH-2′), 74.86 (CH-4), 75.40 (d, J_{PC} = 12 Hz, CH-2′), 75.34 (d, J_{PC} = 16 Hz, CH-3′), 75.68 (dd, J_{PC} = 4 and *ca.* 1 Hz, CH-3′), 76.02 (CH-5), 76.54 (d, J_{PC} = 5 Hz, CH-3), 78.68 (d, $^1J_{PC}$ = 10 Hz, C-1′), 80.32 (d, $^2J_{PC}$ = 17 Hz, C-1), 128.1–129.4 (m, CH of Ph), 132.19, 133.31, 133.39, 135.00 (4 × d, $^2J_{PC}$ = 20 Hz, CH of Ph); 137.25 (d, $^1J_{PC}$ = 12 Hz, C_{ipso} of Ph); 138.16 (virtual t, J_{PC} = 10 Hz, C_{ipso} of Ph), 138.88 (d, $^1J_{PC}$ = 12 Hz, C_{ipso} of Ph), 174.80 (C=O). Note: the assignment for C-1/2 may be interchanged. ^{31}P{^{1}H} NMR ($CDCl_3$): δ −18.2 (s), −18.1 (s). IR (Nujol): ν_{max}/cm^{-1} 1675s, 1583w, 1435s, 1310m, 1282m, 1257m, 1161m, 1070w, 1024w, 841m, 826m, 744vs, 696vs, 480m. MS: *m*/*z* ESI+ 621 ([M + Na]$^+$); ESI− 597 ([M − H]$^-$). HR MS (ESI+) calc. for $C_{35}H_{28}{}^{56}FeO_2P_2Na$ ([M + Na]$^+$) 621.0806, found 621.0827.

Preparation and resolution of 1,2:5,6-di-*O*-isopropylidene-α-D-3-glucofuranosyl 1′,2-bis(diphenylphosphino)ferrocene-1-carboxylates (3). 4-(Dimethylamino) pyridine (0.46 g, 3.73 mmol), 1,2:5,6-di-*O*-isopropylidene-α-D-3-glucofuranose (1.17 g, 4.50 mmol), and *N*,*N*′-dicyclohexylcarbodiimide (0.93 g, 4.50 mmol) were successively added to *rac*-Hdpc (2.23 g, 3.73 mmol) suspended in dichloromethane (120 mL). The resulting red solution was stirred at room temperature for 24 h, filtered and the volatiles were removed under vacuum. The residue was purified by column chromatography on silica gel using hexane–diethyl ether mixture with increasing polarity (4 : 1 → 1 : 1 v/v). The first fraction yielded, after solvent removal, 145 mg (5% yield) of *rac*-4 as a red amorphous solid. Evaporation of the following major band afforded 2.77 g (88%) of a mixture of (R_p)- and (S_p)-**3**. Repeated crystallisation (three times) of this mixture from diethyl ether–hexane afforded analytically pure, orange crystalline (R_p)-**3**. Combined yield of (R_p)-**3**: 1.10 g (35%; 70% of the theoretical amount). The mother liquors from the crystallisations were combined and chromatographed on silica gel (hexane–diethyl ether, 4 : 1 v/v). The mixture of diastereoisomers eluted first (1.28 g, (R_p) : (S_p) ≈ 15 : 85), followed by a second band containing pure (S_p)-**3** (amber glassy solid, 380 mg, 12%).

Analytical data for (R_p)-**3**. Mp 183–186 °C dec. (diethyl ether–hexane). $[\alpha]_D$ +33 (c = 1.0, $CHCl_3$). ^{1}H NMR ($CDCl_3$): δ 1.08 (s, 3 H, C*Me*$_2$), 1.38 (s, 3 H, C*Me*$_2$), 1.42 (s, 6 H, C*Me*$_2$), 3.41 (ddd, J = 2.6, 1.6, 0.9 Hz, CH-3), 3.70 (d, $^3J_{HH}$ = 3.6 Hz, 1 H, CH-2″), 4.02 (d of vq, 1 H, CH-2′), 4.09 (dd, $^3J_{HH}$ = 8.8, 3.2 Hz, 1 H, CH-4″), 4.11 (dd, $^2J_{HH}$ = 8.8, $^3J_{HH}$ = 3.9 Hz, 1 H, CH_2-6″), 4.26 (dd, $^2J_{HH}$ = 8.8, $^3J_{HH}$ = 6.1 Hz, 1 H, CH_2-6″), 4.31 (ddd, $J_1 \approx J_2 \approx$ 2.6, $J_3 \approx$ 0.4 Hz, 1 H, CH-4), 4.32 (d of vq, 1 H, CH-2′), 4.62 and 4.66 (2 × dt, J = 2.4, 1.2 Hz, 1 H, CH-3′); 4.67 (d, $^3J_{HH}$ = 3.6 Hz, 1 H, CH-1″), 4.93 (dddd, $^3J_{HH} \approx$ 9.0, 6.0, 3.8, $J_{PH} \approx$ 3.8 Hz, 1 H, CH-5″), 5.05 (ddd, J = 2.6, 1.6, 0.9 Hz, 1 H, CH-5), 7.09–7.39 (m, 20 H, PPh_2). ^{13}C{^{1}H} NMR ($CDCl_3$): δ 25.55 (C*Me*$_2$, δ_H 1.38), 25.81 (C*Me*$_2$, δ_H 1.08), 26.60 and 27.14 (C*Me*$_2$, δ_H 1.42); 67.80 (CH_2-6″), 72.79 (CH-5″), 74.68 (d, $^1J_{PC}$ = 15 Hz, C-2), 74.80 (d, $^3J_{PC}$ = 3 Hz, CH-4), 75.00 (d, J_{PC} = 13 Hz, CH-2′), 75.08 (d, J_{PC} = 15 Hz, CH-2′), 75.58 (dd, J_{PC} = 4

and 1 Hz, CH-3′), 75.90 (CH-5), 76.02 (d, J_{PC} = 8 Hz, CH-3′), 76.05 (CH-3″), *ca.* 76.9 (CH-3; obscured by the solvent signal), 78.51 (d, $^{1}J_{PC}$ = 10 Hz, C-1′), 79.28 (d, $^{1}J_{PC}$ = 17 Hz, C-1), 80.15 (CH-4″), 83.42 (CH-2″), 104.90 (CH-1″), 109.42 (*C*Me$_2$, C-5a″), 111.63 (*C*Me$_2$, C-1a″), 128.0–129.3 (m, CH of Ph), 132.06 (d, J_{PC} = 19 Hz, CH of Ph), 131.20 (d, J_{PC} = 3 Hz, CH of Ph), 133.40 (d, J_{PC} = 2 Hz, CH of Ph), 135.04 (d, J_{PC} = 22 Hz, CH of Ph), 137.44 (d, $^{1}J_{PC}$ = 13 Hz, C_{ipso} of Ph), 138.21 (d, $^{1}J_{PC}$ = 10 Hz, C_{ipso} of Ph), 139.43 (d, $^{1}J_{PC}$ = 15 Hz, C_{ipso} of Ph), 170.13 (d, $^{3}J_{PC}$ = 3 Hz, C=O). $^{31}P\{^{1}H\}$ NMR ($CDCl_3$): δ −17.9 (s), −15.2 (s). IR (Nujol): ν_{max}/cm^{-1} 1711s, 1584w, 1435s, 1320w, 1262m, 1166w, 1143m, 1071m, 1022m, 842m, 742m, 699m. MS: *m*/*z* ESI+ 841 ($[M + H]^+$), 863 ($[M + Na]^+$). HR MS (ESI+) calc. for $C_{47}H_{46}{}^{56}FeO_7P_2Na$ ($[M + Na]^+$) 863.1960, found 863.1962. Anal. calc. for $C_{47}H_{46}FeO_7P_2$ (840.6): C 67.15, H 5.52%. Found C 66.82, H 5.60%.

Analytical data for (S_p)-**3**. $[\alpha]_D$ −240 (*c* = 1.0, $CHCl_3$). ^{1}H NMR ($CDCl_3$): δ 1.07 (s, 3 H, C(1a″)*Me*$_2$), 1.28 (s, 3 H, C(5a″)*Me*$_2$), 1.36 (s, 3 H, C(5a″)*Me*$_2$), 1.50 (s, 3 H, C(1a″)*Me*$_2$), 3.56 (ddd, $J \approx$ 1.0, 1.5, 2.4 Hz, 1 H, CH-3), 3.75 (m, 1 H, CH-2′), 3.86 (dd, J = 8.5, 5.8 Hz, 1 H, CH-6″), 3.93–4.02 (m, 2 H, CH-5″ and -6″), 4.12 (dd, J = 2.8, 8.8 Hz, 1 H, CH-4″), 4.26 (vt, J = 2.4 Hz, 1 H, CH-4), 4.45 (d, J = 3.4 Hz, 1 H, CH-2″), 4.46 (dt, J = 1.2, 2.4 Hz, 1 H, CH-3′), 4.51 (m, 1 H, CH-2′a), 4.66 (br m, 1 H, CH-3′a), 5.04 (m, 1 H, CH-5), 5.44 (d, J = 2.9 Hz, 1 H, CH-3″), 5.94 (d, J = 3.7 Hz, 1 H, CH-1″), 7.11–7.43 (m, 20 H, PPh_2). $^{13}C\{^{1}H\}$ NMR ($CDCl_3$): δ 25.14 (C*Me*$_2$, δ_H 1.36), 26.32 (C*Me*$_2$, δ_H 1.50), 26.89 (C*Me*$_2$, δ_H 1.28), 27.15 (C*Me*$_2$, δ_H 1.07), 67.37 (CH_2-6″), 71.96 (d, J = 3 Hz, CH-5″), 74.13 (d, $^{2}J_{PC}$ = 7 Hz, CH-2′), 74.54 (d, $^{3}J_{PC}$ = 2 Hz, CH-4), 75.19 (dd, J_{PC} = 2 and 4 Hz, CH-3′), 75.28 (d, $^{1}J_{PC}$ = 16 Hz, C-2), 75.60 (CH-3″), 75.79 (dd, J_{PC} = 2 and 5 Hz, CH-3′a), 75.97 (CH-5), 76.10 (d, $^{2}J_{PC}$ = 20 Hz, CH-2′a), 76.30 (d, $^{2}J_{PC}$ = 5 Hz, CH-3), 78.59 (d, $^{1}J_{PC}$ = 10 Hz, CH-1′), 79.57 (d, $^{2}J_{PC}$ = 18 Hz, CH-1), 80.00 (CH-4″), 83.44 (CH-2″), 105.27 (d, $J_{PC} \approx$ 1 Hz, CH-1″), 109.41 (CH-5a″), 112.38 (CH-1a″), 128.0–128.3 (m, CH of Ph), 128.47, 128.87 , 129.22 (3 × CH of Ph), 132.24, 132.91, 133.71 (3 × d, J_{PC} = 20 Hz, CH of Ph), 135.06 (d, J_{PC} = 22 Hz, CH of Ph), 137.53 (d, J_{PC} = 13 Hz, C_{ipso} of Ph), 137.63, 138.68 (2 × d, J_{PC} = 10 Hz, C_{ipso} of Ph), 139.30 (d, J_{PC} = 12 Hz, C_{ipso} of Ph), 169.39 (d, $^{3}J_{PC}$ = 3 Hz, C=O). $^{31}P\{^{1}H\}$ NMR ($CDCl_3$): δ −18.4 (s), −18.2 (s). IR (Nujol): ν_{max}/cm^{-1} 1719s, 1585w, 1435s, 1324w, 1259m, 1215w, 1163w, 1143m, 1074m, 1025m, 741m, 697m. HR MS (ESI+) calc. for $C_{47}H_{46}{}^{56}FeO_7P_2Na$ ($[M + Na]^+$) 863.1960, found 863.1962.

Analytical data for rac-**4**. ^{1}H NMR ($CDCl_3$): δ 0.90–2.00 (m, 22 H, Cy C*H*$_2$), 3.52 (m, 1 H, NHCy C*H*), 3.72 (m, 1 H, C_5H_3), 3.84 (tt, J = 3.6, 11.9 Hz, 1 H, NCy C*H*), 3.93 (m, 1 H, C_5H_4), 4.17 (dd, $J_1 \approx J_2 \approx$ 2.6 Hz, 1 H, C_5H_3), 4.27 (m, 1 H, C_5H_4), 4.53 (m, 1 H, C_5H_4), 4.59 (m, 1 H, C_5H_4), 4.62 (m, 1 H, C_5H_3), 6. (br d, J = 7.5 Hz, 1H, N*H*), 7.21–7.49 (m, 20 H, 2 × P*Ph*$_2$). $^{13}C\{^{1}H\}$ NMR ($CDCl_3$): δ 24.95, 24.98, 25.26, 25.55, 26.23, 26.43, 30.24, 31.28, 32.57, 33.11 (10 × CH_2 of Cy); 49.86, 58.07 (2 × CH of Cy); 70.91 (CH of Cp), 72.14 (CH of Cp), 74.18 (d, J_{PC} = 4 Hz, CH of Cp), 74.96 (d, J_{PC} = 13 Hz, CH of Cp), 75.96 (d, J_{PC} = 16 Hz, CH of Cp), 76.38 (d, J_{PC} = 7 Hz, C_{ipso} of Cp), 76.44 (d, J_{PC} = 9 Hz, CH of Cp), 77.94 (d, J_{PC} = 10 Hz, CH of Cp), 82.89 (d, J_{PC} = 17 Hz, C_{ipso} of Cp), 84.88 (d, J_{PC} = 16 Hz, C_{ipso} of Cp), 128.1–129.0 (m, CH of Ph), 132.9–133.5 (m, CH of Ph), 133.40 (d, J_{PC} = 21 Hz, CH of Ph), 137.51 (d, J_{PC} = 15 Hz, C_{ipso} of Ph), 138.45 (virtual t, J = 9 Hz, C_{ipso} of Ph), 139.58 (d, J_{PC} = 13 Hz, C_{ipso} of Ph), 154.36 (N*C*(O)N), 170.71 (*C*(O)N). $^{31}P\{^{1}H\}$ NMR ($CDCl_3$): δ −20.6 (s), −17.7 (s). IR (Nujol): ν_{max}/cm^{-1} 3261w, 1699vs, 1626w, 1517m, 1419w, 1316m, 1278w, 1176w, 1136w, 1000w, 832w, 768w, 747m, 696m, 493m. MS: *m*/*z* ESI+ 827 ($[M + Na]^+$), ESI− 678 ($[M - CONHCy]^-$). HR MS (ESI+) calc. for $C_{48}H_{50}{}^{56}FeO_2N_2P_2Na$ ($[M + Na]^+$) 827.2589, found 827.2597.

Preparation of (R_p)- and (S_p)-Hdpc. Glycoside (R_p)-**3** (950 mg, 1.13 mmol) was dissolved in a mixture of THF (30 mL) and methanol (30 mL). Aqueous KOH solution (30 mL of 3 M in degassed water) was added, and the resulting mixture was stirred at 50 °C for 22 h. After cooling to room temperature, the reaction solution was acidified with H_3PO_4 (40% aq. solution). Diethyl ether (30 mL) and brine (30 mL) were added, the organic phase was separated, and the aqueous phase was extracted with diethyl ether (20 mL). The combined extracts were washed with brine (2 × 30 mL), dried over anhydrous $MgSO_4$, and evaporated under vacuum. The residue was dissolved in ethyl acetate, and passed through a short alumina column, eluting with the same solvent. The product remained adsorbed, while the recovered glucose diacetonide eluted. Subsequent elution with methanol–acetic acid mixture (95 : 5 v/v) afforded (R_p)-Hdpc as an orange solid after removal of the solvents (512 mg, 76%). (S_p)-Hdpc was obtained similarly starting from (S_p)-**3** (250 mg, 0.30 mmol) in 69% isolated yield.

Analytical data. (R_p)-Hdpc: $[\alpha]_D$ +189 (*c* = 1.0, $CHCl_3$); (S_p)-Hdpc: $[\alpha]_D$ −187 (*c* = 1.0, $CHCl_3$). NMR and ESI MS spectra of (R_p)- and (S_p)-Hdpc were identical with those of the racemic acid.

When the hydrolysis reaction was carried out at room temperature with 268 mg of (R_p)-**3**, a mixture of products was obtained that, after chromatography (silica gel, dichloromethane–methanol 10 : 1 v/v), gave two fractions. The first fraction (30 mg) contained unreacted (R_p)-**3** and methyl (R_p)-1′,2-bis(diphenylphosphino)ferrocene-1-carboxylate, (R_p)-**5**. Recrystallisation of this fraction from diethyl ether–pentane yielded a mixture of two types of crystals: red prisms and fine yellow needles. The red crystals were manually separated and crystallised once again to yield analytically pure (R_p)-**5**. The second fraction from the chromatography (217 mg) contained the acid and unreacted glycoside, and was processed as described above.

Analytical data for (R_p)-**5**. ^{1}H NMR ($CDCl_3$): δ 3.54 (m, 1 H, C_5H_3), 3.65 (s, 3 H, CO_2Me), 3.91 (m, 1 H, C_5H_4), 4.27 (vt, J = 2.6 Hz, 1 H, C_5H_3), 4.28 (m, 1 H, C_5H_4), 4.49 (m, 2 H, C_5H_4), 4.97 (m, 1 H, C_5H_3), 7.14–7.44 (m, 20 H, 2 × P*Ph*$_2$). $^{31}P\{^{1}H\}$ NMR ($CDCl_3$): δ −17.9 (s), −17.0 (s). IR (Nujol): ν_{max}/cm^{-1} 1714s, 1582w, 1318w, 1309w, 1264m,

1142m, 1067w, 1026w, 829w, 742s, 697s, 478m. HR MS (ESI+) calc. for $C_{36}H_{30}{}^{56}FeO_2P_2Na$ ($[M + Na]^+$) 635.0963, found 635.0959.

General procedure for the preparation of amides 6–10. *N*-[3-(Dimethylamino)propyl]-*N*′-ethylcarbodiimide (0.03 mL, 0.17 mmol) was added to an ice-cooled suspension of (R_p)-Hdpc (54 mg, 0.09 mmol) and 1-hydroxybenzotriazole (15 mg, 0.1 mmol) in dichloromethane (5 mL). After 5 min, a solution of the appropriate amine (1.2 equiv.) in the same solvent (1–2 mL) was introduced and the mixture was stirred at room temperature for 20 h. Then, the reaction solution was diluted with dichloromethane (10 mL); extracted successively with 1 M HCl (5 mL), saturated aqueous hydrogen carbonate (10 mL), and brine (10 mL); dried ($MgSO_4$); and evaporated under vacuum. The products were isolated by column chromatography (silica gel, dichloromethane–methanol 20 : 1 v/v) and obtained as orange glassy solids after evaporation. The yields were typically very good ($\geq 95\%$), the exceptions being the 2-hydroxyethyl ((R_p)-**10**, 78%) and diphenylmethyl ((R_p)-**9**, 65%) amides. In the latter case, intermediate benzotriazolyl ester (R_p)-**11** was also isolated (31%).

(R_p)-1′,2-Bis(diphenylphosphino)-1-(*N*-isopropyl-carbamoyl)-ferrocene, (R_p)-6. Prepared from isopropylamine (7 mg). Yield: 55 mg (96%). $[\alpha]_D$ +203 (c = 1.0, $CHCl_3$). ^1H NMR ($CDCl_3$): δ 0.98, 1.21 (2 × d, ^3J = 6.5 Hz, 3 H, CH*Me*$_2$), 3.53 (m, 1 H, C_5H_3), 3.75 (m, 1 H, C_5H_4), 4.10 (m, 1 H, C*H*Me$_2$), 4.26 (vt, J = 2.6 Hz, 1 H, C_5H_3), 4.27 (m, 1 H, C_5H_4), 4.37, 4.42 (2 × m, 1 H, C_5H_4), 4.99 (m, 1 H, C_5H_3), 6.89 (dd, J = 8.1, 10.9 Hz, 1 H, N*H*), 7.10–7.48 (m, 20 H, 2 × P*Ph*$_2$). $^{31}P\{^1H\}$ NMR ($CDCl_3$): δ −20.1 (s), −17.8 (s). IR (RAS): ν_{max}/cm^{-1} 3321w br, 1648vs, 1526s, 1478m, 1434s, 1266m, 1163m, 1026w, 834w, 741vs, 696vs, 487m. HR MS (ESI+) calc. for $C_{38}H_{36}{}^{56}FeNOP_2$ ($[M + H]^+$) 640.1616, found 640.1598.

(R_p)-1′,2-Bis(diphenylphosphino)-1-(*N*-benzyl-carbamoyl)-ferrocene, (R_p)-7. Prepared from benzylamine (12 mg). Yield: 60 mg (97%). $[\alpha]_D$ +188 (c = 1.0, $CHCl_3$). ^1H NMR ($CDCl_3$): δ 3.59 (m, 1 H, C_5H_3), 3.67, 4.22 (2 × m, 1 H, C_5H_4), 4.30–4.34 (m, 3 H, C_5H_3 and C_5H_4), 4.50 (d, J = 5.8 Hz, 2 H, NHCH_2Ph), 5.05 (m, 1 H, C_5H_3), 7.06–7.46 (m, 26 H, 2 × P*Ph*$_2$, CH$_2$*Ph*, and N*H*). $^{13}C\{^1H\}$ NMR ($CDCl_3$): δ 43.60 (*C*H$_2$Ph), 73.68 (d, J = 2 Hz, *C*H of Cp), 73.97 (m, *C*H of Cp), 75.01 (d, J = 4 Hz, *C*H of Cp), 75.40 (d, J = 6 Hz, *C*H of Cp), 75.77 (d, J = 17 Hz, *C*H of Cp), 76.19 (d, J = 11 Hz, C_{ipso} of Cp), 78.09 (d, J = 10 Hz, C_{ipso} of Cp), 81.21 (d, J = 18 Hz, C_{ipso} of Cp), 127.11, 127.61 (2 × *C*H of Ph), 128.1–128.7 (m, *C*H of Ph), 129.68 (*C*H of Ph), 132.10 (d, J = 17 Hz, *C*H of Ph), 133.12, 133.53 (2 × d, J = 20 Hz, *C*H of Ph), 135.04 (d, J = 21 Hz, *C*H of Ph), 135.79 (d, J = 7 Hz, C_{ipso} of Ph), 137.89 (d, J = 10 Hz, C_{ipso} of Ph), 137.93 (d, J = 7 Hz, C_{ipso} of Ph), 138.51 (d, J = 10 Hz, C_{ipso} of Ph), 138.68 (C_{ipso} of Ph), 169.54 (d, $^3J_{PC}$ = 4 Hz, *C*ONH). $^{31}P\{^1H\}$ NMR ($CDCl_3$): δ −20.4 (s), −17.9 (s). IR (Nujol): ν_{max}/cm^{-1} 3319w br, 1651m, 1633s, 1585w, 1544m composite, 1275w, 1161w, 1027w, 836w, 743s, 697vs, 498m. HR MS (ESI+) calc. for $C_{42}H_{35}{}^{56}FeNOP_2Na$ ($[M + Na]^+$) 710.1436, found 710.1434.

(R,R_p)-1′,2-Bis(diphenylphosphino)-1-[*N*-(1-phenyl-ethyl)-carbamoyl]-ferrocene, (R,R_p)-8. Prepared from (*R*)-(1-phenyl-ethyl)amine (13 mg). Yield: 61 mg (97%). $[\alpha]_D$ +150 (c = 1.0, $CHCl_3$). ^1H NMR ($CDCl_3$): δ 1.30 (d, ^3J = 7.0 Hz, 3 H, CH*Me*Ph), 3.53 (m, 1 H, C_5H_3), 3.64, 4.12, 4.18, 4.29 (4 × m, 1 H, C_5H_4), 4.30 (vt, J = 2.6 Hz, 1 H, C_5H_3), 5.05 (m, 1 H, C_5H_3), 5.14 (m, 1 H, C*H*MePh), 7.12–7.48 (m, 25 H, 2 × P*Ph*$_2$, and *Ph*), 7.59 (dd, J = 8.2, 12.8 Hz, 1 H, N*H*). $^{31}P\{^1H\}$ NMR ($CDCl_3$): δ −20.3 (s), −17.8 (s). IR (RAS): ν_{max}/cm^{-1} 3306w br, 1648s, 1585w, 1523s, 1478m, 1434s, 1263w, 1160m, 743vs, 697vs, 486m. HR MS (ESI+) calc. for $C_{43}H_{38}{}^{56}FeNOP_2$ ($[M + H]^+$) 702.1773, found 702.1757.

(S,R_p)-1′,2-Bis(diphenylphosphino)-1-[*N*-(1-phenyl-ethyl)-carbamoyl]-ferrocene, (S,R_p)-8. Prepared from (*S*)-(1-phenyl-ethyl)amine (13 mg). Yield: 60 mg (95%). $[\alpha]_D$ +184 (c = 1.0, $CHCl_3$). ^1H NMR ($CDCl_3$): δ 1.54 (d, ^3J = 6.8 Hz, 3 H, CH*Me*Ph), 3.53 (m, 1 H, C_5H_3), 3.74, 4.23 (2 × m, 1 H, C_5H_4), 4.28 (vt, J = 2.6 Hz, 1 H, C_5H_3), 4.39 (m, 2 H, C_5H_4), 5.05 (m, 1 H, C_5H_3), 5.19 (m, 1 H, C*H*MePh), 7.01–7.46 (m, 26 H, 2 × P*Ph*$_2$, CHMe*Ph*, and N*H*). $^{31}P\{^1H\}$ NMR ($CDCl_3$): δ −20.4 (s), −17.9 (s). IR (RAS): ν_{max}/cm^{-1} 3315w br, 1636s, 1523s, 1478m, 1433s, 1263m, 1160m, 1026m, 836w, 741vs, 695vs, 487m. HR MS (ESI+) calc. for $C_{43}H_{38}{}^{56}FeNOP_2$ ($[M + H]^+$) 702.1773, found 702.1766.

(R_p)-1′,2-Bis(diphenylphosphino)-1-(*N*,*N*-diphenyl-methyl-carbamoyl)ferrocene, (R_p)-9. Starting with amino(diphenyl)-methane (21 mg), the general procedure furnished a mixture of products whose chromatographic separation (silica gel, dichloromethane–methanol 50 : 1 v/v) gave two bands. After evaporation, the first band afforded benzotriazolyl ester (R_p)-**11** (20 mg) and the second one provided pure amide (R_p)-**9** (45 mg, 65%). $[\alpha]_D$ +191 (c = 1.0, $CHCl_3$). ^1H NMR ($CDCl_3$): δ 3.52 (m, 1 H, C_5H_3), 3.64, 4.07, 4.15, 4.27 (4 × m, 1 H, C_5H_4), 4.33 (vt, J = 2.6 Hz, 1 H, C_5H_3), 5.13 (m, 1 H, C_5H_3), 6.34 (dd, J = 2.5, 8.6 Hz, 1 H, NHC*H*Ph$_2$), 6.99–7.44 (m, 30 H, 2 × P*Ph*$_2$, and CH*Ph*$_2$), 8.07 (dd, J = 8.5, 13.1 Hz, 1 H, N*H*). $^{31}P\{^1H\}$ NMR ($CDCl_3$): δ −20.7 (s), −17.9 (s). IR (RAS): ν_{max}/cm^{-1} 3300w br, 1655s, 1585w, 1514s composite, 1434s, 1267w, 1159m, 1027m, 909m, 836w, 742vs, 700vs, 489s. HR MS (ESI+) calc. for $C_{48}H_{40}{}^{56}FeNOP_2$ ($[M + H]^+$) 764.1929, found 764.1928.

(R_p)-1′,2-Bis(diphenylphosphino)-1-[*N*-(2-hydroxyethyl)-carbamoyl]ferrocene, (R_p)-10. Prepared as described above from (2-hydroxyethyl)amine (7 mg). Yield: 45 mg (78%). $[\alpha]_D$ +267 (c = 1.0, $CHCl_3$). ^1H NMR ($CDCl_3$): δ 2.74 (br s, 1 H, O*H*), 3.45 (q, J = 5.1 Hz, 2 H, CH_2), 3.60–3.70 (m, 3 H, C_5H_3, and CH_2), 3.71 (m, 1 H, C_5H_4), 4.30–4.34 (m, 3 H, C_5H_3, and C_5H_4), 4.42 (m, 1 H, C_5H_4), 5.01 (m, 1 H, C_5H_3), 7.10–7.49 (m, 21 H, 2 × P*Ph*$_2$, and N*H*). $^{31}P\{^1H\}$ NMR ($CDCl_3$): δ −20.3 (s), −18.3 (s). IR (Nujol): ν_{max}/cm^{-1} 3293w br, 1629s, 1583w, 1531s, 1435vs, 1338m, 1307m, 1274m, 1160m, 1026m, 834w, 741vs, 695vs, 488m. HR MS (ESI+) calc. for $C_{37}H_{34}{}^{56}FeNOP_2$ ($[M + H]^+$) 642.1409, found 642.1409; calc. for $C_{37}H_{33}{}^{56}FeNNaOP_2$ ($[M + Na]^+$) 664.1228, found 664.1225.

Analytical data for (R_p)-11. ^{1}H NMR ($CDCl_3$): δ 3.85 (m, 1 H, C_5H_3), 4.08 (m, 1 H, C_5H_4), 4.54–4.57 (m, 2 H, C_5H_3, and C_5H_4), 4.71, 4.93 (2 × m, 1 H, C_5H_4), 5.24 (m, 1 H, C_5H_3), 6.94–6.97 (m, 1 H, $C_6H_4N_3$), 7.15–7.48 (m, 22 H, 2 × PPh_2 and $C_6H_4N_3$), 7.99–8.02 (m, 1 H, $C_6H_4N_3$). $^{31}P\{^1H\}$ NMR ($CDCl_3$): δ −18.4 (s), −18.1 (s). IR (RAS): ν_{max}/cm^{-1} 1782s, 1478w, 1434m, 1249w, 1087m, 1021w, 906w, 744vs, 698vs, 500m. HR MS (ESI+) calc. for $C_{41}H_{32}{}^{56}FeN_3O_2P_2$ ($M + H^+$) 716.1314, found 716.1312.

Dichlorido-[*rac*-1′,2-bis(diphenylphosphino)-ferrocene-1-carboxylic acid-κ^2*P*,*P*′]palladium(II) (12). A solution of *rac*-Hdpc (12 mg, 0.02 mmol) in chloroform (2 mL) was layered with a solution of $[PdCl_2(cod)]$ (5.7 mg, 0.02 mmol) in the same solvent (1 mL). After standing at room temperature for two days, the deposited solid was filtered off and dried under vacuum to give **12** as an orange microcrystalline solid (12 mg, 77%). Crystals of **12**·Me_2CO (**12a**) were obtained similarly by using acetone as the solvent for $[PdCl_2(cod)]$.

^{1}H NMR (DMSO-d_6): δ 3.69 (m, 1 H, C_5H_3), 4.03 (m, 1 H, C_5H_4), 4.42 (m, 2 H, C_5H_3 and C_5H_4), 4.52 (m, 1 H, C_5H_4), 4.57 (m, 1 H, C_5H_4), 5.19 (m, 1 H, C_5H_3), 7.25–8.20 (m, 20 H, 2 × PPh_2). $^{31}P\{^1H\}$ NMR (DMSO-d_6): δ 33.5 (d, $^2J_{PP}$ = 35 Hz), 43.7 (d, $^2J_{PP}$ = 35 Hz). IR (Nujol): ν_{max}/cm^{-1} 3347w br, 1703vs, 1680w, 1307w, 1257w, 1192w, 1148m, 1094m, 835w, 749m, 698s, 554m, 497m, 469m. MS: *m*/*z* ESI+ 739 ($[M - Cl]^+$), 761 ($[M + Na - HCl]^+$). Anal. calc. for $C_{35}H_{28}FePdO_2P_2Cl_2$·0.15$CHCl_3$ (793.6): C 53.20, H 3.58%. Found C 53.02, H 3.50%.

Preparation of (η^3-1,3-diphenylallyl){(*R*$_p$)-1′,2-bis(diphenylphosphino)-1-(*N*-benzylcarbamoyl)ferrocene-κ^2*P*,*P*′}palladium(II) perchlorate, (R_p)-16. A suspension of amide (R_p)-**7** (14 mg, 20 μmol) and **15** (6.7 mg, 10 μmol) in dichloromethane (3 mL) was stirred at room temperature for 15 min, yielding a clear solution. A solution of $AgClO_4$ in acetonitrile (0.1 mL of 0.2 M solution, 0.02 mmol) was then added and stirring was continued for 1 h. The formed precipitate (AgCl) was filtered off (PTFE syringe filter, 0.45 μm pore size) and the filtrate was evaporated under vacuum to yield (R_p)-**16** as a yellow solid (21 mg).

^{1}H NMR ($CDCl_3$): δ 3.48 (m, 1 H, C_5H_4), 3.96 (m, 1 H, C_5H_4), 4.13 (m, 1 H, C_5H_3), 4.26 (m, 1 H, C_5H_4), 4.36 (vt, *J* = 2.8 Hz, 1 H, C_5H_3), 4.65–4.75 (m, 3 H, CH_2Ph, C*H* allyl, and C_5H_4), 5.20–5.33 (m, 2 H, CH_2Ph, and C*H* allyl), 5.64 (m, 1 H, C_5H_3), 6.45–7.70 (m, 26 H, 5 × Ph, and C*H*-*meso* allyl), 8.38 (dd, *J* = 5.0 Hz, 6.8 Hz, 1 H, N*H*). $^{13}C\{^1H\}$ NMR ($CDCl_3$); selected signals: δ 72.19 (d, *J* = 6 Hz), 73.10 (d, *J* = 5 Hz), 73.66 (d, *J* = 6 Hz), 74.13 (d, *J* = 10 Hz), 75.23 (d, *J* = 4 Hz), 79.34 (d, *J* = 7 Hz), 81.40 (d, *J* = 11 Hz) (7 × CH of ferrocene moiety); 91.16 (d, *J* = 26 Hz, *C*H allyl), 93.63 (d, *J* = 23 Hz, *C*H allyl), 110.68 (m, *C*H-*meso* allyl), 170.04 (CO). $^{31}P\{^1H\}$ NMR ($CDCl_3$): δ 21.3, 30.0 (2 × d, $^2J_{PP}$ = 61 Hz, *P*Ph$_2$). IR (Nujol): ν_{max}/cm^{-1} 3356w br, 1628m, 1582w, 1536m, 1438s, 1339w, 1270w, 1165w, 1096vs composite, 1028w, 747m, 694s, 624m, 493m. IR (0.02 M in $CDCl_3$): ν_{max}/cm^{-1} 3366w br, 1625m, 1540m, 1437m, 1271w, 1097s. MS: *m*/*z* ESI+ 986 ($[M - ClO_4]^+$), 793 ($[M - ClO_4 - Ph_2C_3H_3]^+$). HR MS (ESI+) calc. for $C_{57}H_{48}{}^{56}FeNOP_2Pd$ (the cation) 986.1590, found 986.1613.

Asymmetric allylic alkylation—general procedure

Ligand (8 μmol), $[\{Pd(\eta^3\text{-}C_3H_5)Cl\}_2]$ (1.5 mg, 4 μmol), and alkali metal acetate (16 μmol; if appropriate) were mixed with dry dichloromethane (3 mL) and the mixture was stirred at room temperature for 30 min. Allylic substrate (0.25 mmol; 63 mg of **13a** or 71 mg of **13b**) was introduced and followed, after stirring for another 5 min, successively with *N*,*O*-bis(trimethylsilyl)acetamide (BSA; 0.19 mL, 0.75 mmol) and malonate (0.75 mmol; 0.09 mL of dimethyl malonate or 0.17 mL of di-*tert*-butyl malonate). The resulting mixture was stirred for 20 h and washed with saturated aqueous NH_4Cl (2 × 5 mL). The organic layer was separated, dried over $MgSO_4$ and concentrated under vacuum. Purification by column chromatography (silica gel; hexane–ethyl acetate 3 : 1 v/v) afforded the alkylation product (or its mixture with unreacted substrate in the case of incomplete conversion).

Enantiomeric excesses were determined from integration of ^{1}H NMR spectra recorded in C_6D_6 in the presence of tris(3-trifluoroacetyl-*d*-camphorato)europium(III). Configuration of the major enantiomer was assigned on the basis of optical rotation of the mixture.[50]

X-Ray crystallography. Crystals suitable for X-ray diffraction analysis were grown from hot aqueous acetic acid (*rac*-Hdpc: orange needle, 0.10 × 0.15 × 0.40 mm), diethyl ether–pentane ((R_p)-**5**: orange prism, 0.40 × 0.43 × 0.50 mm), diethyl ether–hexane ((R_p)-**3**: orange needle, 0.05 × 0.08 × 0.27 mm), and from warm ethyl acetate ((R_p)-**16a**: orange block, 0.06 × 0.12 × 0.21 mm). Crystals of **12a** were selected directly from the reaction batch (orange plate, 0.08 × 0.15 × 0.25 mm).

The diffraction data ($\pm h \pm k \pm l$; $2\theta \leq 50.8°$ for (R_p)-**3**, 55° for other compounds) were collected with a Nonius KappaCCD diffractometer equipped with a Cryostream Cooler (Oxford Cryosystems) using graphite monochromatised MoKα radiation (λ = 0.71073 Å). The solvent molecules in the structure of (R_p)-**16a** were disordered and, hence, their contribution to the overall diffraction intensity was removed by the SQUEEZE routine[51] incorporated in the PLATON program.[52]

The structures were solved by direct methods (SIR97[53]) and refined by full-matrix least squares procedure based on F^2 (SHELXL97[54]). The non-hydrogen atoms were refined with anisotropic displacement parameters. Carboxylic hydrogens (H2) in the structures of *rac*-Hdpc and **12a** were located on electron density maps and refined as riding atoms. All other hydrogen atoms were included in their calculated positions and refined as riding atoms. Selected crystallographic data are given in Table 6. Geometric parameters and structural drawings were obtained with a recent version of the PLATON program. The calculated values are rounded with respect to their estimated uncertainties (esd's) given with one decimal; parameters involving atoms in calculated positions are given without esd's.

Table 6 Crystallographic data, data collection and structure refinement parameters for *rac*-Hdpc, (R_p)-**5**, (R_p)-**3**, **12a**, and (R_p)-**16a**

Compound	*rac*-Hdpc	(R_p)-**5**	(R_p)-**3**	**12a**	(R_p)-**16a**
Formula	$C_{35}H_{28}FeO_2P_2$	$C_{36}H_{30}FeO_2P_2$	$C_{47}H_{46}FeO_7P_2$	$C_{38}H_{34}Cl_2FeO_3P_2Pd$[d]	$C_{65}H_{64}ClFeNO_9P_2Pd$[f]
M/g mol^{-1}	598.36	612.39	840.63	833.74	1262.81
Crystal system	Monoclinic	Monoclinic	Monoclinic	Triclinic	Monoclinic
Space group	$P2_1/c$ (no. 14)	$P2_1$ (no. 4)	$C2$ (no. 5)	$P\bar{1}$ (no. 2)	$P2_1$ (no. 4)
T/K	150(2)	150(2)	150(2)	150(2)	150(2)
a/Å	9.0484(2)	9.0257(2)	34.878(1)	10.7792(2)	13.0501(7)
b/Å	17.9216(3)	17.9691(3)	8.5038(2)	10.9451(2)	14.616(1)
c/Å	8.8899(2)	9.0278(2)	14.9636(4)	16.5867(3)	16.703(1)
α/°	—	—	—	70.8340(9)	—
β/°	95.942(1)	94.440(1)	110.062(1)	82.3917(9)	111.357(5)
γ/°	—	—	—	68.1648(9)	—
V/Å^3	1433.86(5)	1459.77(5)	4168.8(2)	1715.69(5)	2967.2(3)
Z	2	2	4	2	2
D_{calc}/g mL^{-1}	1.386	1.393	1.339	1.614	1.413
μ(Mo Kα)/mm^{-1}	0.669	0.659	0.490	1.234[e]	0.704[g]
Diffractions total	22442	22122	28497	48729	21194
Unique/obsd[a] diffrns	3284/2721	6607/6300	7640/6905	7885/6876	11769/9534
R_{int}(%)[b]	3.3	3.6	5.2	3.8	4.2
R (observed data) (%)[c]	3.47	3.88	3.31	2.86	4.93
R, wR (all data) (%)[c]	4.52, 9.25	3.14, 8.30	4.17, 7.18	3.64, 6.83	6.81, 10.9
Flack's parameter	NA	0.02(1)	−0.01(1)	NA	0.00(2)
$\Delta\rho$/e Å^{-3}	0.39, −0.32	0.57, −0.52	0.38, −0.27	1.09, −0.67	0.69, −0.60
CCDC entry	700753	700754	700755	700756	700757

[a] Diffractions with $I_o > 2\sigma(I_o)$ were regarded as observed. [b] $R_{int} = \Sigma|F_o^2 - F_o^2(\text{mean})|/\Sigma F_o^2$, where F_o^2(mean) is the average intensity of symmetry-equivalent diffractions. [c] $R = \Sigma||F_o| - |F_c||/\Sigma|F_o|$, w$R = [\Sigma\{w(F_o^2 - F_c^2)_2\}/\Sigma w(F_o^2)^2]^{1/2}$. [d] $C_{35}H_{28}Cl_2FeO_2P_2Pd{\cdot}C_3H_6O$. [e] Corrected for absorption; range of transmission coefficients = 0.738–0.904. [f] $[C_{57}H_{48}FeO_5P_2Pd]ClO_4{\cdot}2C_4H_8O_2$. [g] Corrected for absorption; range of transmission coefficients = 0.911–0.965.

Acknowledgements

We thank Dr A. Růžička and Dr Z. Padělková for recording the X-ray diffraction data for (R_p)-**16a**. This work is a part of research projects supported by the Ministry of Education of the Czech Republic (project nos. MSM0021620857 and LC06070).

References

1 G. P. Sollot, J. L. Snead, S. Portnoy, W. R. Peterson and H. E. Mertwoy, *U. S. Department of Commerce, Office of Technical Services, PB Report*, 1965, vol. II, pp. 441–452 (Chem. Abstr., 1965, **63**, 18174).

2 (*a*) S. W. Chien and T. S. A. Hor, *The Coordination and Homogenous Catalytic Chemistry of 1,1′-Bis(diphenylphosphino)-ferrocene and its Chalcogenide Derivatives*, in *Ferrocenes: Ligands, Materials and Biomolecules*, ed. P. Štěpnička, Wiley, Chichester, 2008, ch. 2, pp. 33–116; (*b*) T. J. Colacot, *Platinum Met. Rev.*, 2001, **45**, 22; (*c*) G. Bandoli and A. Dolmella, *Coord. Chem. Rev.*, 2000, **209**, 161; (*d*) K.-S. Gan and T. S. A. Hor, *1,1′-Bis(diphenylphosphino)ferrocene—Coordination Chemistry, Organic Syntheses, and Catalysis*, in *Ferrocenes: Homogeneous Catalysis, Organic Synthesis, Materials Science*, ed. A. Togni and T. Hayashi, VCH, Weinheim, 1995, ch. 1, pp. 3–104.

3 T. J. Colacot and S. Parisel, *Synthesis, Coordination Chemistry and Catalytic Use of dppf Analogs*, in *Ferrocenes: Ligands, Materials and Biomolecules*, ed. P. Štěpnička, Wiley, Chichester, 2008, ch. 3, pp. 117–140.

4 (*a*) H.-U. Blaser, W. Chen, F. Camponovo and A. Togni, *Chiral 1,2-Disubstituted Ferrocene Diphosphines for Asymmetric Catalysis*, in *Ferrocenes: Ligands, Materials and Biomolecules*, ed. P. Štěpnička, Wiley, Chichester, 2008, ch. 6, pp. 205–235; (*b*) P. Štěpnička and M. Lamač, *Synthesis and Catalytic Use of Planar Chiral and Polydentate Ferrocene Donors*, in *Ferrocenes: Ligands, Materials and Biomolecules*, ed. P. Štěpnička, Wiley, Chichester, 2008, ch. 7, pp. 237–277; (*c*) R. C. J. Atkinson, V. C. Gibson and N. J. Long, *Chem. Soc. Rev.*, 2004, **33**, 313; (*d*) T. J. Colacot, *Chem. Rev.*, 2003, **103**, 3101; (*e*) A. Togni, *New Chiral Ferrocenyl Ligands for Asymmetric Catalysis*, in *Metallocenes*, ed. A. Togni, R. L. Halterman, Wiley-VCH, Weinheim, 1998, vol. 2, ch. 11, pp. 685–721; (*f*) T. Hayashi, *Asymmetric Catalysis with Chiral Ferrocenylphosphine Ligands*, in *Ferrocenes: Homogeneous Catalysis, Organic Synthesis, Materials Science*, ed. A. Togni, T. Hayashi, VCH, Weinheim, 1995, ch. 2, pp. 105–142.

5 D. Marquarding, H. Klusacek, G. Gokel, P. Hoffmann and I. Ugi, *J. Am. Chem. Soc.*, 1970, **92**, 5389.

6 (*a*) T. Hayashi, K. Yamamoto and M. Kumada, *Tetrahedron Lett.*, 1974, **15**, 4405; (*b*) T. Hayashi, T. Mise, S. Mitachi, K. Yamamoto and M. Kumada, *Tetrahedron Lett.*, 1976, **17**, 1133.

7 T. Hayashi, T. Mise, M. Fukushima, M. Kagotani, N. Nagashima, Y. Hamada, A. Matsumoto, S. Kawakami, M. Konishi, K. Yamamoto and M. Kumada, *Bull. Chem. Soc. Jpn.*, 1980, **53**, 1138.

8 (*a*) T. Hayashi, *Pure Appl. Chem.*, 1988, **60**, 7; (*b*) T. Hayashi and M. Kumada, *Acc. Chem. Res.*, 1982, **15**, 395; (*c*) See also ref. 4*c*–*f*,36*f*.

9 (*a*) I. R. Butler and W. R. Cullen, *Organometallics*, 1986, **5**, 2537; (*b*) I. R. Butler, L. J. Hobson, S. M. E. Macan and D. J. Williams, *Polyhedron*, 1993, **12**, 1901; (*c*) I. R. Butler, S. Müssig and M. Plath, *Inorg. Chem. Commun.*, 1999, **2**, 424.

10 (*a*) O. B. Sutcliffe and M. R. Bryce, *Tetrahedron: Asymmetry*, 2003, **14**, 2297; (*b*) C. J. Richards and A. J. W. Locke, *Tetrahedron: Asymmetry*, 1998, **9**, 2377; (*c*) L.-X. Dai, T. Tu, S.-L. You, W.-P. Deng and X.-L. Hou, *Acc. Chem. Res.*, 2003, **36**, 659.

11 P. Štěpnička, *Eur. J. Inorg. Chem.*, 2005, 3787.

12 (*a*) M. Lamač, I. Císařová and P. Štěpnička, *Eur. J. Inorg. Chem.*, 2007, 2274; (*b*) P. Štěpnička, J. Schulz, I. Císařová and K. Fejfarová, *Collect. Czech. Chem. Commun.*, 2007, **72**, 453; (*c*) J. Kühnert, M. Dušek, J. Demel, H. Lang and P. Štěpnička, *Dalton Trans.*, 2007, 2802; (*d*) J. Kühnert, M. Lamač, T. Rüffer, B. Walfort, P. Štěpnička and H. Lang, *J. Organomet. Chem.*, 2007, **692**, 4303; (*e*) C. Bianchini, A. Meli, W. Oberhauser, A. M. Segarra, E. Passaglia, M. Lamač and P. Štěpnička, *Eur. J. Inorg. Chem.*, 2008, 441; (*f*) J. Kühnert, M. Lamač, J. Demel, A. Nicolai, H. Lang and P. Štěpnička, *J. Mol. Catal. A: Chem.*, 2008, **285**, 41; (*g*) J. Kühnert, I. Císařová, M. Lamač and P. Štěpnička, *Dalton Trans.*, 2008, 2454.

13 J. Podlaha, P. Štěpnička, I. Císařová and J. Ludvík, *Organometallics*, 1996, **15**, 543.

14 (*a*) S.-L. You, X.-L. Hou, L.-X. Dai, B.-X. Dao and J. Sun, *Chem. Commun*., 2000, 1933; (*b*) J. M. Longmire, B. Wang and X. Zhang, *Tetrahedron Lett*., 2000, **41**, 5435; (*c*) P. Štěpnička, *New J. Chem*., 2002, **26**, 567; (*d*) B. Breit and D. Breuninger, *Synthesis*, 2005, 2782.

15 For applications, see: (*a*) ref. 14*a–b*; (*b*) S.-L. You, Y.-M. Luo, W.-P. Deng, X.-L. Hou and L.-X. Dai, *J. Organomet. Chem*., 2001, **637–639**, 845; (*c*) M. Lamač, J. Tauchman, I. Císařová and P. Štěpnička, *Organometallics*, 2007, **26**, 5042; (*d*) S.-L. You, X.-L. Hou and L.-X. Dai, *J. Organomet. Chem*., 2001, **637–639**, 762; (*e*) S.-L. You, X.-L. Hou, L.-X. Dai and X.-Z. Zhu, *Org. Lett*., 2001, **3**, 149; (*f*) J. M. Longmire, B. Wang and X. Zhang, *J. Am. Chem. Soc*., 2002, **124**, 13400; (*g*) B. Breit and D. Breuninger, *J. Am. Chem. Soc*., 2004, **126**, 10244; (*h*) B. Breit and D. Breuninger, *Eur. J. Org. Chem*., 2005, 3916; (*i*) B. Breit and D. Breuninger, *Synthesis*, 2005, 147.

16 Only esters and amides of **IV** are known: (*a*) W. Zhang, T. Kida, Y. Nakatsuji and I. Ikeda, *Tetrahedron Lett*., 1996, **37**, 7995; (*b*) W. Zhang, T. Shimanuki, T. Kida, Y. Nakatsuji and I. Ikeda, *J. Org. Chem*., 1999, **64**, 6247; (*c*) R. S. Laufer, U. Veith, N. J. Taylor and V. Snieckus, *Org. Lett*., 2000, **2**, 629.

17 For examples of the resolution of carboxylic acids *via* D-glucose diacetonide esters, see: (*a*) J. Svoboda, K. Čapek and J. Paleček, *Collect. Czech. Chem. Commun*., 1987, **52**, 766; (*b*) A. Netscher and I. Gautschi, *Liebigs Ann. Chem*., 1992, 543; (*c*) O. I. Kolodiazhnyi and E. V. Griskun, *Tetrahedron: Asymmetry*, 1996, **7**, 967.

18 M. Lamač, J. Cvačka and P. Štěpnička, *J. Organomet. Chem*., 2008, **693**, 3430.

19 Column chromatography is usually not sufficient for a complete separation of the diastereoisomers, affording only mixtures with gradually increasing (S_p)-**3**/(R_p)-**3** ratios. Chromatography combined with crystallisation is a much more efficient resolution method.

20 B. Schetter and B. Speiser, *J. Organomet. Chem*., 2004, **689**, 1472.

21 ^{1}H NMR data: (*a*) A. De Bruyn, D. Danneels, M. Anteunis and E. Saman, *J. Carbohydr., Nucleosides Nucleotides*, 1975, **2**, 227; ^{13}C NMR data: (*b*) D. M. Vyas, H. C. Jarrell and W. A. Szarek, *Can. J. Chem*., 1973, **53**, 2748.

22 The observed distance is comparable with the sum of the van der Waals radii (2.89 Å). The radii were taken from the CCDC web site: http://www.ccdc.cam.ac.uk/products/csd/radii/ (retrieved on August 5, 2008).

23 H.-B. Kraatz, *J. Inorg. Organomet. Polym. Mater*., 2005, **15**, 83.

24 For examples involving ferrocene phosphinocarboxylic acids, see: (*a*) Ref. 12*a–c*, *f*, *g*; (*b*) L. Meca, D. Dvořák, J. Ludvík, I. Císařová and P. Štěpnička, *Organometallics*, 2004, **23**, 2541.

25 Formation of the related Hdpf-benzotriazolyl ester was noted during the reaction of Hdpf with 1,2-diaminoethane in the presence of EDC and HOBt (see ref. 12*b*).

26 Dppf crystallises with the symmetry of the monoclinic space group $P2_1/a$ with the Fe atom residing on the inversion centre.

27 U. Casellato, D. Ajo, G. Valle, B. Corain, B. Longato and R. Graziani, *J. Crystallogr. Spectrosc. Res*., 1988, **18**, 583.

28 P. Štěpnička and I. Císařová, *New J. Chem*., 2002, **26**, 567.

29 The difference between P1-C2-C(1/3) angles is *ca.* 3° while the C(5/2)-C1-C11 and P2-C6-C(7/10) angles differ by *ca.* 7° in the pairs. The pivotal phosphorus atoms (P1 and P2) are displaced by *ca.* 0.1 Å from the least-squares planes of their bonding cyclopentadienyl rings. By contrast, the C11 atom is coplanar with the Cp1 ring within 0.01 Å and the carboxyl group is rotated by 8° from the Cp1 plane.

30 (*a*) W. H. Ojala, W. B. Gleason, M. P. E. Connelly and R. R. Wallis, *Acta Crystallogr., Sect. C: Cryst. Struct. Commun*., 1996, **52**, 155; (*b*) J. Sheville, D. Berndt, T. Wagner and P. Norris, *J. Chem. Crystallogr*., 2003, **33**, 409.

31 The differences are below *ca.* 0.1 Å for the bond lengths and typically *ca.* 2–3° for the angles.

32 T. Hayashi, M. Konishi, Y. Kobori, M. Kumada, T. Higuchi and K. Hirotsu, *J. Am. Chem. Soc*., 1984, **106**, 158.

33 I. R. Butler, W. R. Cullen, J.-T. Kim, S. J. Rettig and J. Trotter, *Organometallics*, 1985, **4**, 972.

34 Pd, Cl2, P1, and P2 are coplanar within *ca.* 0.02 Å. The remaining donor atom, Cl1, is displaced by 0.163(1) Å from the least-squares plane comprising these atoms, moved away from the carboxyl group.

35 The Cp rings are tilted by 2.3(2)° and bind symmetrically to the iron atom (Δ(Fe–Cg) = 0.014 Å). The asymmetry in functional group attachment is diminished compared to free Hdpc (Δ ≈ 1° for C(2/5)-C1-C11, and Δ ≈ 1° for C(1/3)-C2-P1 and C(7/10)-C6-P2 angles).

36 (*a*) B. M. Trost and D. L. Van Vranken, *Chem. Rev*., 1996, **96**, 395; (*b*) B. M. Trost and M. L. Crawley, *Chem. Rev*., 2003, **103**, 2921; (*c*) B. M. Trost and C. Lee, *Asymmetric Allylic Alkylation Reactions*, in *Catalytic Asymmetric Synthesis*, ed. I. Ojima, Wiley-VCH, New York, 2nd edn, 2000, ch. 8E, pp. 593–650; (*d*) G. Helmchem and A. Pfaltz, *Acc. Chem. Res*., 2000, **33**, 336; (*e*) G. Helmchem, *J. Organomet. Chem*., 1999, **576**, 203; (*f*) T. Hayashi, *Asymmetric Allylic Substitution and Grignard Cross-Coupling*, in *Catalytic Asymmetric Synthesis*, ed. I. Ojima, VCH, New York, 1993, ch. 7.1, pp. 325-365.

37 (*a*) U. Leutenegger, G. Umbricht, C. Fahrni, P. von Matt and A. Pfaltz, *Tetrahedron*, 1992, **48**, 2143; (*b*) B. M. Trost and D. J. Murphy, *Organometallics*, 1985, **4**, 1143; (*c*) M. T. El Gihani and H. Heaney, *Synthesis*, 1998, 357.

38 Definition: ee = ([*R*] − [*S*])/([*R*] + [*S*]). Positive ee values indicate that (*R*)-**15** is the dominant product.

39 For introductory reviews, see: (*a*) C. Girard and H. B. Kagan, *Angew. Chem., Int. Ed*., 1998, **37**, 2922; (*b*) H. B. Kagan, *Synlett*, 2001, 888.

40 For selected examples of (η^3-allyl)palladium(II) complexes with *P*,*P*-chelating ferrocene ligands, see: (*a*) P. Barbaro, P. S. Pregosin, R. Salzmann, A. Albinati and R. W. Kunz, *Organometallics*, 1995, **14**, 5160; (*b*) U. Burckhardt, V. Gramlich, P. Hofmann, R. Nesper, P. S. Pregosin, R. Salzmann and A. Togni, *Organometallics*, 1996, **15**, 3496; (*c*) S.-L. You, X.-L. Hou, L.-X. Dai, Y.-H. Yu and W. Xia, *J. Org. Chem*., 2002, **67**, 4684; (*d*) T. Tu, Y.-G. Zhou, X.-L. Hou, L.-X. Dai, X.-C. Dong, Y.-H. Yu and J. Sun, *Organometallics*, 2003, **22**, 1255; (*e*) T. Sturm, B. Abad, W. Weissensteiner, K. Mereiter, B. R. Manzano and F. A. Jalón, *J. Organomet. Chem*., 2006, **225**, 209; (*f*) C.-W. Cho, J.-H. Son and K.-H. Ahn, *Tetrahedron: Asymmetry*, 2006, **17**, 2240.

41 U. Nettekoven, M. Widhalm, H. Kalchhauser, P. C. J. Kamer, P. W. N. M. van Leeuwen, M. Lutz and A. L. Spek, *J. Org. Chem*., 2001, **66**, 759.

42 (*a*) C. A. Hunter and J. K. M. Sanders, *J. Am. Chem. Soc*., 1990, **112**, 5525. See also: (*b*) C. A. Hunter, K. R. Lawson, J. Perkins and C. J. Urch, *J. Chem. Soc., Perkin Trans. 2*, 2001, 651.

43 The centroid···centroid distance in hexagonal graphite (space group $P6_3/mmm$) is *ca.* 3.65 Å. P. Trucano and R. Chen, *Nature*, 1975, **258**, 136.

44 (*a*) F. O. Rice and E. Teller, *J. Chem. Phys*., 1938, **6**, 489 (erratum: F. O. Rice and E. Teller, *J. Chem. Phys*., 1939, **7**, 199); (*b*) J. Hine, *Adv. Phys. Org. Chem*., 1977, **15**, 1.

45 In the presence of BSA, the carboxyl group of the free acid ligand can be expected to be (at least partially) converted to the silyl ester.

46 This was already demonstrated for 1′,2-bis(phosphine)-1-oxazolinylferrocenes. T. Tu, X.-L. Hou and L.-X. Dai, *J. Organomet. Chem*., 2004, **689**, 3847.

47 Acetate **14a** was prepared by acetylation of commercial racemic 1,3-diphenylallyl alcohol: I. D. G. Watson, S. A. Styler and A. K. Yudin, *J. Am. Chem. Soc*., 2004, **126**, 5086.

48 F. Ferioli, C. Fiorelli, G. Martelli, M. Monari, D. Savoia and P. Tobaldin, *Eur. J. Org. Chem*., 2005, 1416.

49 T. Hayashi, A. Yamamoto, Y. Ito, E. Nishioka, H. Miura and K. Yanagi, *J. Am. Chem. Soc*., 1989, **111**, 6301.

50 T. Hayashi, A. Yamamoto, T. Hagihara and Y. Ito, *Tetrahedron Lett*., 1986, **27**, 191.

51 P. van der Sluis and A. L. Spek, *Acta Crystallogr., Sect. A: Fundam. Crystallogr*., 1990, **46**, 194.

52 A. L. Spek, *Platon—a multipurpose crystallographic tool*, Utrecht University, Utrecht, The Netherlands, 2003 and updates. For reference, see: A. L. Spek, *J. Appl. Crystallogr*., 2003, **36**, 7.

53 A. Altomare, M. C. Burla, M. Camalli, G. L. Cascarano, C. Giacovazzo, A. Guagliardi, A. G. G. Moliterni, G. Polidori and R. Spagna, *J. Appl. Crystallogr*., 1999, **32**, 115.

54 G. M. Sheldrick, *SHELXL97. Program for Crystal Structure Refinement from Diffraction Data*, University of Göttingen, Germany, 1997.

